

HOMOGENEOUS HYDROGENATION CATALYSED BY SQUARE
PLANAR IRIDIUM (I) COMPLEXES

by

NAZIR AHMED MEMON

B.Sc. (Hons), University of Sind, W. Pakistan, 1963

M.Sc., University of Sind, W. Pakistan, 1964

A THESIS SUBMITTED IN PARTIAL FULFILMENT OF
THE REQUIREMENTS FOR THE DEGREE OF
MASTER OF SCIENCE

in the Department
of
CHEMISTRY

We accept this thesis as conforming to the
required standard

THE UNIVERSITY OF BRITISH COLUMBIA

July, 1967

In presenting this thesis in partial fulfilment of the requirements for an advanced degree at the University of British Columbia, I agree that the Library shall make it freely available for reference and Study. I further agree that permission for extensive copying of this thesis for scholarly purposes may be granted by the Head of my Department or by his representatives. It is understood that copying or publication of this thesis for financial gain shall not be allowed without my written permission.

Department of CHEMISTRY

The University of British Columbia
Vancouver 8, Canada

Date July 28, 1967.

ABSTRACT

A study is described of the kinetics of reactions in which the complexes $\text{trans-Ir(CO)X(PPh}_3)_2$, where $X = \text{Cl, Br and I}$, are used for the catalytic homogeneous hydrogenation of olefins, in particular maleic acid. The catalytic activity is poor in benzene solutions but is enhanced in coordinating solvents such as N, N' -dimethylacetamide. The kinetics were studied by measurements of hydrogen uptake at various experimental conditions in which iridium, olefin and hydrogen concentrations were varied.

The rate-law is complex showing between zero and first order in each of iridium, substrate and hydrogen concentrations. The dependence of rate on the halogen followed the order $\text{I} > \text{Br} > \text{Cl}$, and quite remarkably traces of oxygen in the system enhance the hydrogenation rate considerably. Supplementary spectrophotometric studies have elucidated some of the equilibria involved and the mechanisms proposed show the importance of a solvent assisted dissociation step in making available a coordination site on the transition metal complex.

A detailed path for the catalytic hydrogenation is suggested.

ACKNOWLEDGEMENT

I feel great pleasure in expressing my deep sense of indebtedness and gratitude to Dr. B.R. James, under whose patient guidance this work was carried out.

Financial assistance from the University of British Columbia Graduate Fellowship programme is gratefully acknowledged.

TABLE OF CONTENTS

CHAPTER	PAGE
I. INTRODUCTION	1
(A) General Aim of the Work	1
(B) Homogeneous Catalytic Hydrogenation	1
(i) Inorganic substrates	2
(ii) Catalytic hydrogenation of olefin substrates	3
(C) Literature Reports of Iridium Complexes as Hydrogenation Catalysts	8
(D) Oxidative-Additions and Related Reactions of Iridium (I) Complexes	10
II. EXPERIMENTAL PROCEDURE	13
(A) Iridium Complexes	13
(B) Other Materials	14
(C) Apparatus for Constant Pressure Gas Uptake Measurements	15
(D) Procedure	16
(E) Spectrophotometric Measurements	18
III. RESULTS OF GAS UPTAKE MEASUREMENTS	23
1. Ir(CO)Cl(PPh ₃) ₂ Systems	23
2. Ir(CO)Br(PPh ₃) ₂ Systems	33
3. Ir(CO)I(PPh ₃) ₂ Systems	34
4. Ethylene as Substrate	34

CHAPTER	PAGE
5. Effect of Oxygen on Rates of Hydrogenation .	40
IV. SPECTROPHOTOMETRIC RESULTS	41
1. $\text{Ir}(\text{CO})\text{Cl}(\text{PPh}_3)_2/\text{H}_2$ Equilibrium	41
2. $\text{Ir}(\text{CO})\text{Cl}(\text{PPh}_3)_2$ Solutions Without Sub- strates	43
3. Complexing with Maleic Acid	46
V. DISCUSSION	51
APPENDIX	60
REFERENCES	62

LIST OF TABLES

TABLE	PAGE
I. Variation of Rate with $\text{Ir}(\text{CO})\text{Cl}(\text{PPh}_3)_2$ Concentration	25
II. Variation of Rate with $\text{Ir}(\text{CO})\text{Cl}(\text{PPh}_3)_2$ Concentration; Using Stock Solution Left at 80° Overnight	25
III. Variation of Rate with $\text{Ir}(\text{CO})\text{Cl}(\text{PPh}_3)_2$ Concentration; Using Stock Solution Left at Room Temp. for 10 Days	26
IV. Variation of Rate with Maleic Acid Concentration	26
V. Variation of Rate with Hydrogen Pressure	27
VI. Variation of Rate with Hydrogen Pressure; Using Stock Solution Left at Room Temp. for 10 Days	27
VII. Effect of Adding Various Reagents on the Rate	28
VIII. Variation of Rate with $\text{Ir}(\text{CO})\text{Cl}(\text{PPh}_3)_2$ Concentration, Using Fumaric Acid as Substrate	28
IX. Variation of Rate with $\text{Ir}(\text{CO})\text{Cl}(\text{PPh}_3)_2$ Concentration (in DMSO)	35
X. Variation of Rate with $\text{Ir}(\text{CO})\text{Br}(\text{PPh}_3)_2$ Concentration	35

TABLE	PAGE
XI. Variation of Rate with Maleic Acid, Using Bromo Complex	36
XII. Variation of Rate with Hydrogen Pressure, Using Bromo Complex	36
XIII. Variation of Rate with $\text{Ir}(\text{CO})\text{I}(\text{PPh}_3)_2$ Concentration	37
XIV. Variation of Rate with Maleic Acid Concentration; Using Iodo Complex	37
XV. Variation of Rate with Hydrogen Pressure; Using Iodo Complex	38
XVI. Summarized Results for Maleic Acid Complex Formation	49b
XVII. Summary of the Hydrogenation Data at 80°	56

LIST OF FIGURES

FIGURE	PAGE
1. Reaction Scheme for Hydrogenation of Olefin by Chlororuthenate (II) Complexes	4
2. Reaction Scheme for Hydrogenation of Olefins by $\text{RhCl}(\text{PPh}_3)_3$ Complex	6
3. The Hydrogenation Apparatus	21
4. Reaction Cell for Spectrophotometric Studies	22
5. A Typical Hydrogen Uptake Plot	29
6. Effect of Variation of $\text{Ir}(\text{CO})\text{Cl}(\text{PPh}_3)_2$ Conc. on the Uptake Plots	30
7. Variation of Rate with $\text{Ir}(\text{CO})\text{Cl}(\text{PPh}_3)_2$ Concentration	31
8. Variation of Rate with Maleic Acid Concentration	31
9. Variation of Rate with Hydrogen Pressure	32
10. Effect of Variation of $\text{Ir}(\text{CO})\text{Cl}(\text{PPh}_3)_2$ Conc. on Uptake Plots when Fumaric Acid is used as Substrate	39
11. Spectrum of $\text{Ir}(\text{CO})\text{Cl}(\text{PPh}_3)_2$	42
12. Plots of Optical Density against Time for "Blanks"	44
13. Plot of $\text{Log } A/B$ against Time for the "Blank" at 25°	44

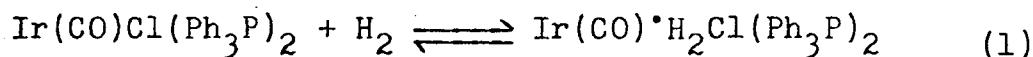
FIGURE	PAGE
14. Plots of Optical Density against Time for Maleic Acid Complexing at Different Conditions	50
15. Plots of Log $\frac{O.D_o^2 - O.D_t O.D_e}{O.D_o (O.D_t - O.D_e)}$ against Time .	50

I. INTRODUCTION

(A) General aim of the work

The aim of the work described in this thesis is to investigate the potentiality of the iridium complexes, trans-Ir(CO)X(Ph₃P)₂ (where X = halogen) as hydrogenation catalysts for the reduction of simple organic substrates in solution. Where such activation of molecular hydrogen has been observed, the detailed kinetics of the reactions have been studied with a view to elucidating the mechanisms involved.

The interest in the present work arose from the fact that trans-chloro-carbonyl bis(triphenyl phosphine)Ir(I) was reported a few years ago by Vaska and DiLuzio¹ to react reversibly with hydrogen to form a molecular dihydride:



It seemed possible that in such a system the hydrogen molecule might be activated for chemical reaction.

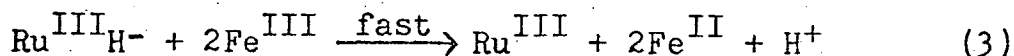
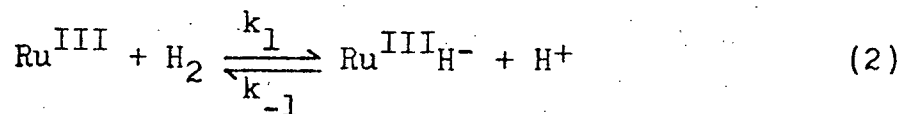
(B) Homogeneous catalytic Hydrogenation

The study of catalytic properties of transition metal complexes, particularly of Group VIII metal ions has attracted a great deal of interest in the past few years. Two recent reviews by Halpern^{2,3} which covered the literature up to the

end of 1964 have concerned themselves with a variety of reactions including homogeneous hydrogenation. Very recently two important papers dealing with detailed kinetic studies of a ruthenium (II) catalysed hydrogenation system⁴ and a rhodium (I) catalysed system⁵ have been published.

(i) Inorganic Substrates

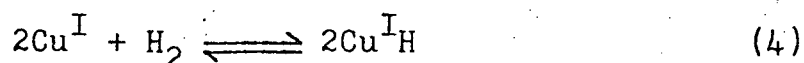
The mechanism of these reactions involves a rate-determining heterolytic or homolytic splitting of molecular hydrogen by the catalytic species; this results in the formation of an intermediate metal hydride species which reduces the substrate in a subsequent fast reaction. An example involving the heterolytic splitting of the hydrogen molecule is seen in the ruthenium (III) catalysed reduction of Fe^{III} which can be represented as follows:^{6,7}



The rate-law is $-\text{d}[\text{H}_2]/\text{dt} = k_1[\text{H}_2][\text{Ru}^{\text{III}}]$, which becomes pseudo-first order if the gas uptake measurements are made at constant pressure.

A system involving homolytic splitting of hydrogen is the copper (I) catalysed hydrogen reduction of copper (II) in quinoline solution⁸ in which the observed rate-law is $-\text{d}[\text{H}_2]/\text{dt} = k[\text{H}_2][\text{Cu}^{\text{I}}]^2$, consistent with the rate-determining

step being



Other metal ion complexes found to activate hydrogen for the reduction of inorganic substrates by these mechanisms include those of Copper (II), Silver (I), Rhodium (III), Palladium (II) and Cobalt (II)². There has been no report of iridium complexes catalysing the hydrogen reduction of inorganic substrates. Halpern⁹ reports that Iridium (III) is not active but gives no detail of the investigation.

(ii) Catalytic Hydrogenation of Olefinic Substrates

Among metal complexes which activate molecular hydrogen, only a few appear to be effective catalysts for the homogeneous hydrogenation of olefinic compounds. These have all been reported quite recently in about the last six years, and include complexes of Ruthenium (II)^{4,10}, Platinum (II)¹¹, Cobalt (II)^{12,13}, Rhodium (III)⁵, Rhodium (I)^{5,14}, Cobalt (I)¹⁵ and Iron (0)¹⁶. Since the present work was started, Vaska has briefly reported^{17,18} that some Iridium (I) complexes including the ones that we were studying were also active.

Detailed kinetic studies have been reported on three of these systems involving Ruthenium (II)⁴, Rhodium (I)⁵, and Cobalt (II)¹². It is worthwhile to consider each of these, since each differs slightly in the proposed mechanisms of the hydrogenation and hence present a good comparison of the various possible mechanisms.

Halpern, Harrod and James^{4,10} have reported that the hydrogenation of olefinic carboxylic acids such as maleic and fumaric acids catalysed by chlororuthenate (II) complexes in acidified aqueous solutions takes place via an initial rapid formation of a 1:1 Ru (II) olefin π -complex followed by reaction of this π -complex with hydrogen in the rate-determining step. The mechanism is depicted as follows:

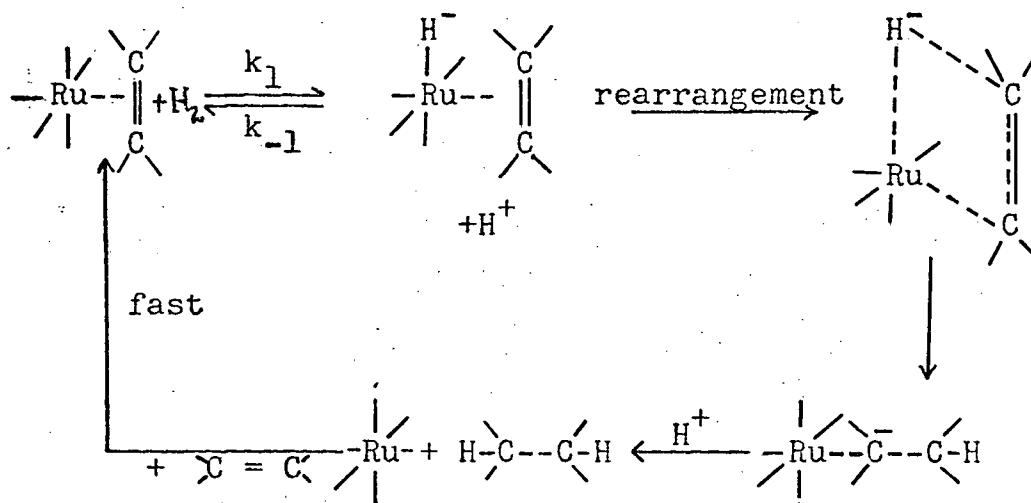


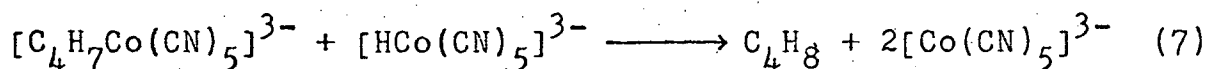
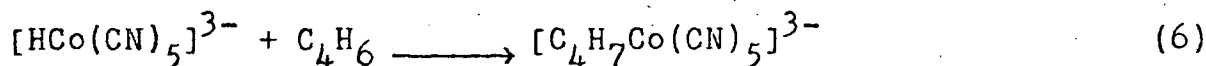
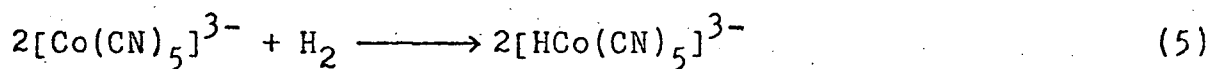
Figure 1

The rate law for this scheme is

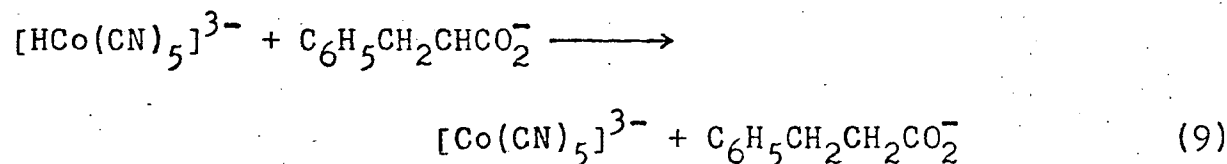
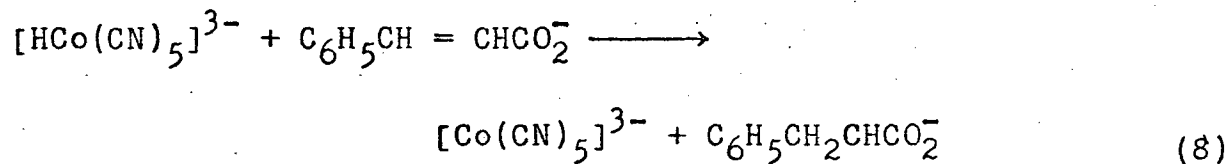
$$-\frac{d[\text{H}_2]}{dt} = k_1[\text{H}_2][\text{Ru}^{\text{II}}(\text{olefin})]$$

The olefinic substrate itself is thus activated as well as the hydrogen molecule by coordination to the metal ion. Simple olefins such as ethylene and propylene although forming π -complexes with Ru^{II} were not hydrogenated; a carboxyl substituent adjacent to the double bond is required for the hydrogen reduction. It is suggested that this is associated with the rearrangement step involving nucleophilic attack of the hydride ligand on the double bond.

Kwiatek, Mador and Seyler¹² have reported that pentacyano cobalt (II), $\text{Co}(\text{CN})_5^{3-}$, is a homogeneous catalyst for the hydrogenation of certain conjugated olefins such as butadiene, styrene, cinnamic acid, etc. Again simple mono-olefins and non-conjugated dienes were not hydrogenated. The mechanism proposed for hydrogenation of butadiene is as follows:



The intermediate $[\text{C}_4\text{H}_7\text{Co}(\text{CN})_5]^{3-}$ has also been prepared and characterized by Kwiatek and Seyler¹⁹. Simandi and Nagi¹³ suggested, however, that the $\text{Co}(\text{CN})_5^{3-}$ catalysed hydrogenation of cinnamate ($\text{PhCH}=\text{CHCO}_2^-$) involved a radical-anion intermediate:



Wilkinson et al⁵ have recently reported that chloro, tris-(triphenyl phosphine) rhodium (I) in benzene solution

is an active catalyst for homogeneous hydrogenation of a variety of olefinic compounds (but not ethylene itself). An important feature of the catalysis involves the dissociation of the $\text{RhCl}(\text{Ph}_3\text{P})_3$ complex in solution to give a solvated species $\text{RhCl}(\text{Ph}_3\text{P})_2(\text{S})$, (where S = solvent), which has a site for coordination of the olefin or hydrogen by displacement of the solvent, and separate reactions with both molecular hydrogen and ethylene have yielded the crystalline derivatives $\text{RhCl}(\text{PPh}_3)_2\text{H}_2$ and $\text{RhCl}(\text{PPh}_3)_2\text{C}_2\text{H}_4$. The system is summarized in the following reaction scheme:

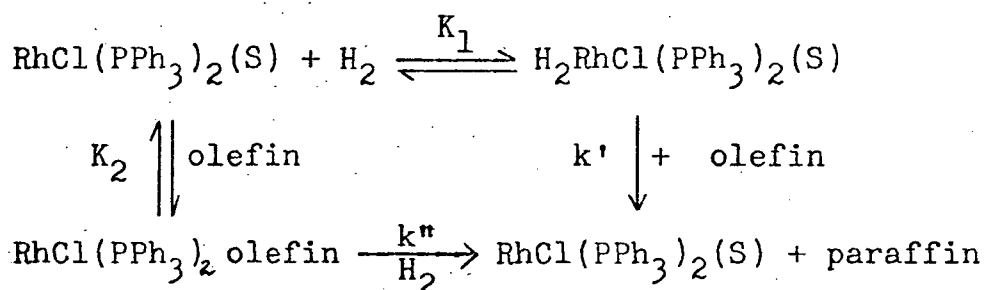


Figure 2

The authors have shown that the attack of hydrogen on the olefin complex does not occur, which leaves the formation of paraffin solely due to attack of the olefin on the dihydride complex formed in an initial rapid equilibrium. The uncomplexed olefin is thought to attack the dihydride at the vacant site to give a transition state in which both hydrogen and olefin are bound to the metal. The rate-law of this mechanistic scheme is

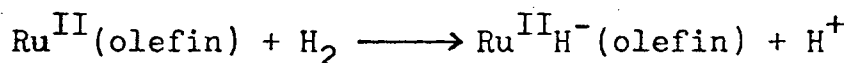
$$\text{Rate} = \frac{k'K_1p[\text{Y}][\text{RhCl}(\text{PPh}_3)_2(\text{S})]}{1 + K_1p + K_2[\text{Y}]}$$

where Y = substrate and p = concentration of hydrogen in solution.

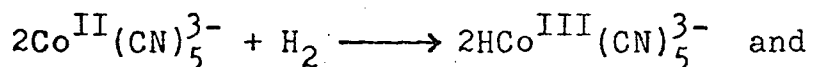
Related and of interest is a report by James and Rempel¹⁴ that rhodium trichloride trihydrate in dimethylacetamide solution is an efficient catalyst for the homogeneous hydrogenation of ethylene itself as well as substituted ethylenes such as maleic acid. Kinetic studies indicate that hydrogen initially reduces Rhodium (III) to the univalent state which rapidly forms a complex with the olefin substrate and the mechanism is thought to be similar to that for the Ruthenium (II) catalysed system (figure 1).

In each of the above cases hydrido metallic species are indicated as reaction intermediates and Halpern² has suggested that the catalytic activity of the hydride complex is controlled by its thermodynamic stability and lability; that is, if the intermediate is unstable it will not be formed readily while if its stability is too great its subsequent transformation to the products will be slow. Three routes are thus recognized for the formation of the hydrido intermediates during the hydrogenation of the olefin:

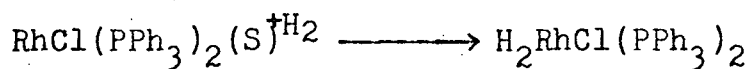
(a) heterolytic splitting of hydrogen, e.g.,



(b) homolytic splitting of hydrogen, e.g.,



(c) addition of hydrogen to form a dihydride, e.g.,



An interesting feature of these olefin hydrogenation reactions is whether both of the reactants (hydrogen, olefin) or just the hydrogen need to be activated by the central metal atom. The Rhodium (I) and Cobalt (II) systems indicate the latter whereas the olefin in the Ruthenium (II) system is undoubtedly activated as well. All three mechanisms at some stage involve the addition of a metal hydride to the olefin, i.e.,



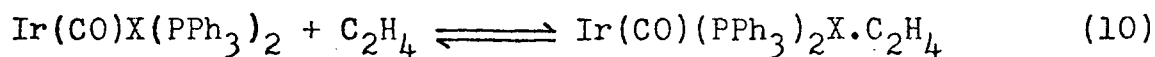
and many such hydrometallation reactions have been observed directly, e.g., with $\text{HPtCl}(\text{PEt}_3)_2$ ^{20,21}, $\text{HMn}(\text{CO})_5$ ²², $\text{HCo}(\text{CN})_5$ ²³, $[\text{RhH}(\text{CN})_4\text{H}_2\text{O}]^{2-}$ ²⁴ and $\text{RhHCl}_2(\text{PPh}_3)_2$ ²⁵. No examples in iridium chemistry have so far been reported. Hydrometallation is an example of a much wider class of "insertion"-type reactions recently discussed by Heck²⁶ whose general widespread role in catalytic reaction has also been considered.³

(C) Literature Reports of Iridium Complexes as Hydrogenation Catalysts

The discovery of the $\text{Ir}(\text{CO})\text{Cl}(\text{PPh}_3)_2$ complex by Vaska and DiLuzio¹ reported in 1962 and its reactions with

molecular hydrogen¹ (equation 1) presumably led Vaska and coworkers to investigate the possible activity of this complex as a hydrogenation catalyst. Two short communications on such studies were published at the end of 1965.^{17,18} James and McLaughlin²⁷ had started solution studies in this laboratory early that year and the work described in this thesis is a continuation of their work.

Vaska and coworkers^{17,18} reported that the complexes $\text{Ir}(\text{CO})(\text{PPh}_3)_2\text{X}$ (X = halogen) and $\text{IrH}(\text{CO})(\text{PPh}_3)_3$ do act as catalysts in benzene and toluene solutions for homogeneous hydrogenation of ethylene and acetylene, the complexes reacting reversibly with the olefin or acetylene as well as molecular hydrogen, e.g.,



Detailed kinetics were not reported and possible mechanisms were not discussed; however, the catalytic systems were very inefficient e.g., with a 10^{-3} M solution of $\text{Ir}(\text{CO})\text{Cl}(\text{PPh}_3)_2$, hydrogen pressures up to 1 atmosphere and ethylene pressure of 1/2 atmosphere at 60° , a maximum 40% yield of ethane was obtained after 18 hours.

James and McLaughlin²⁷ found that hydrogenation of hex-1 ene and cyclohexene using the $\text{Ir}(\text{CO})\text{Cl}(\text{PPh}_3)_2/\text{H}_2$ system in benzene solution was extremely slow and not practical for kinetic studies. Styrene was reduced somewhat more rapidly, the data obtained at 50° and constant hydrogen

pressure, fitted the rate-law:

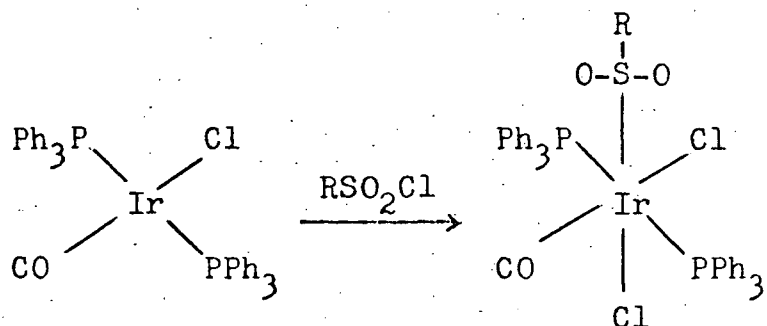
$$-d[\text{H}_2]/dt = k'[\text{styrene}][\text{Ir}(\text{CO})\text{Cl}(\text{PPh}_3)_2]_{\text{initial}}$$

with $k' \approx 4.0 \times 10^{-2} \text{ l mole}^{-1} \text{ sec}^{-1}$. A few other preliminary experiments indicated that catalytic activity of $\text{Ir}(\text{CO})\text{Cl}(\text{PPh}_3)_2$ was considerably enhanced in dimethylacetamide solution using maleic acid as a convenient substrate. There was also some spectrophotometric evidence that complexing occurred between the maleic acid and the iridium complex. The kinetics of the reaction of hydrogen with the iridium complex in benzene solution at 25°C were found to be first order in the complex and for experiments at constant hydrogen pressure a pseudo first order rate constant of $2.0 \times 10^{-3} \text{ sec}^{-1}$ was estimated. This result is in good agreement with some very recently published work by Halpern and Chock²⁸ who have carried out a much more detailed study of this reaction.

(D) Oxidative-Additions and Related Reactions of Iridium (I) complexes

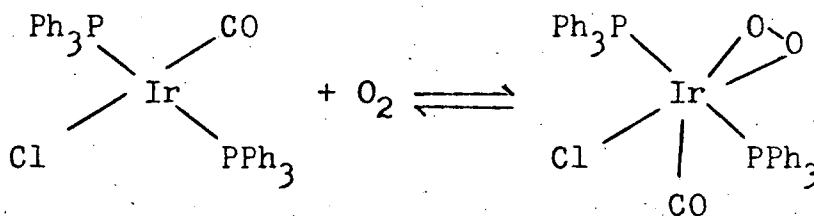
Complexes such as $\text{Ir}(\text{CO})\text{X}(\text{PPh}_3)_2$ of d^8 -configuration undergo the now familiar oxidative-addition reactions by adding a wide variety of covalent molecules to form hexacoordinated complexes of d^6 -configuration and considerable literature has recently appeared dealing with such chemistry.^{29,30} This is relevant and will be briefly reviewed. In the product of reaction (1) the hydrogen is thought to be present as two anionic hydride ligands occupying normal cis-coordination

positions in the Ir^{III} complex.¹ Vaska and Diluzio first reported that covalent molecules such as halogens (X₂), hydrogen halides (HX), organic halides (RX) readily add to give the compounds Ir(CO)X₃(PPh₃)₂, IrH(CO)X₂(PPh₃)₂ and Ir(CO)R(PPh₃)₂X₂ respectively. Collman and coworkers²⁹ have more recently reported the addition of alkyl and aryl sulphonyl chlorides to give iridium (III) sulphinates:



Mercuric halides also add to give derivatives³¹ containing Ir-Hg metal bonds in compounds such as (Ph₃P)₂(CO)Cl₂Ir-HgCl. Acid azides, RCON₃, may add similarly to give an unstable species with two nitrogen atoms occupying octahedral positions; the product isolated is, however, the novel molecular nitrogen complex, Ir(CO)Cl(Ph₃P)₂N₂.³²

The Ir(CO)Cl(PPh₃)₂ complex also takes up molecular oxygen reversibly³³



The structure of the peroxo complex has been confirmed by X-ray analysis.³⁴ The ethylene complex (reaction 10) is by analogy assumed to contain the $[\text{C}_2\text{H}_4]^-$ ion.¹⁸ Similarly extensive σ -bonding in the closely related tetrafluoroethylene³⁵ and tetracyanoethylene³⁶ complexes is thought to predominate rather than the alternative of π -bonding in a 5-coordinated iridium (I) complex. Collman and Kang³² have recently reported the preparation of acetylene complexes. The compounds obtained by the reversible addition of CO ³⁷ and SO_2 ³⁰ to $\text{Ir}(\text{CO})\text{Cl}(\text{PPh}_3)_2$ have recently been described, and the introduction of a methylene group into the complex using diazomethane has been reported.³⁸

Detailed kinetic studies of the addition of hydrogen, oxygen, and methyl iodide to the $\text{Ir}(\text{CO})\text{X}(\text{PPh}_3)_2$ complexes in benzene and DMF solutions have been reported by Halpern and Chock.²⁹ The reactions were first order in each reactant and followed a simple bimolecular rate law, i.e.,

$$-d[\text{Ir}(\text{CO})\text{X}(\text{PPh}_3)_2]/dt = k[\text{Ir}(\text{CO})\text{X}(\text{PPh}_3)_2][\text{YZ}]$$

where $\text{YZ} = \text{H}_2, \text{O}_2$ or CH_3I . The observed decrease in the concentration of $\text{Ir}(\text{CO})\text{X}(\text{PPh}_3)_2$ will obey a pseudo-first order rate law if the concentrations of YZ are kept constant. The rate constants and activation parameters are reported. It is found that the reactivity of the iridium complexes towards oxygen and hydrogen in benzene solutions decreased in the sequence: $\text{Ir}(\text{CO})\text{I}(\text{PPh}_3)_2 > \text{Ir}(\text{CO})\text{Br}(\text{PPh}_3)_2 > \text{Ir}(\text{CO})\text{Cl}(\text{PPh}_3)_2$ and that the reaction rates increased in more polar solvent, DMF.

II. EXPERIMENTAL PROCEDURE

(A) Iridium Complexes

Trans-chlorocarbonyl-bis (triphenylphosphine) iridium (I) was first prepared by Vaska and DiLuzio¹ by refluxing $\text{IrCl}_3(\text{H}_2\text{O})_x$ or $(\text{NH}_4)_2\text{IrCl}_6$ and triphenylphosphine in alcohols for several hours. This procedure resulted in complexes containing carbonyl and/or hydride ligands from which the square planar diamagnetic $\text{Ir}^{\text{I}}(\text{CO})\text{Cl}(\text{PPh}_3)_2$ could be isolated; mpt. 323-325^o; ν_{CO} 1950 cm^{-1} . Small amounts of this complex had been prepared using this method in this laboratory by McLaughlin, and were used for some of the earlier experiments in the present studies. The method of preparation, however, was found to be rather unreproducible and a commercial sample recently marketed by Johnson Matthey and Co. was subsequently used; the properties were identical with those of the laboratory prepared material.

The corresponding bromo and iodo compounds were prepared by exchange reactions according to the methods recently described by Chock and Halpern.²⁹ Trans-bromocarbonyl-bis-(triphenylphosphine) iridium (I) was prepared by dissolving $\text{Ir}(\text{CO})\text{Cl}(\text{PPh}_3)_2$ in tetrahydrofuran and adding a ten-fold excess of LiBr. After standing for one hour the solution was evaporated to dryness, the residue extracted with water (to remove LiCl and excess LiBr) and the water insoluble

product recrystallized from benzene. Trans-Ir(CO)I(PPh₃)₂ was prepared by dissolving Ir(CO)Cl(PPh₃)₂ in benzene, adding a tenfold excess of NaI in ethanol, shaking the mixture for one hour in the dark, and then evaporating to dryness. The residue was shaken with benzene-water mixture, and the benzene layer was separated and evaporated to dryness; the product was recrystallized from benzene and stored in the dark. Both the bromo and iodo compounds were prepared under a nitrogen atmosphere. The carbonyl stretching frequencies agreed with those reported in the literature²⁹ (Ir(CO)Br(PPh₃)₂, $\nu_{\text{CO}} = 1955 \text{ cm}^{-1}$ and Ir(CO)I(PPh₃)₂, $\nu_{\text{CO}} = 1975 \text{ cm}^{-1}$).

(B) Other Materials

Purified hydrogen and nitrogen were obtained from Canadian Liquid Air Co.; the hydrogen was passed through a "deoxo" catalytic purifier to remove traces of oxygen before use. Carbon monoxide and ethylene were obtained as C.P. grade (99.5%) from Matheson Co. Maleic and fumaric acids were of C.P. grade from Eastman Kodak and were recrystallized from water and water/ethanol respectively before use. (Their purity was checked by melting point determination.) N, N-Dimethylacetamide (b.p. 165°-166°) used as solvent in these studies was obtained from Eastman Organic Chemicals (Kodak) and was further distilled under reduced pressure before use (60°, 15 mm). The benzene used was of spectroscopic grade

obtained from Fisher Scientific Company. All other chemicals used were of reagent grade.

(C) Apparatus for Constant Pressure Gas-Uptake Measurements

The apparatus used for some kinetic studies involves the measurement of gas-uptake at constant pressure, e.g., during hydrogenation of various substrates, and it is shown in figure 3 (page 21)

The capillary manometer M could be connected to a double-neck reaction flask E by a spring coil arrangement Q at the tap N. The reaction flask could be immersed in a silicone oil-bath O thermostated at the desired temperature and shaken by means of the shaking device P. The gas-burette K (containing some mercury) and the connected capillary manometer were maintained at 25° C using a thermostated water-bath.

The gas-burette was connected through the tap H and the needle valve G to the mercury manometer R which in turn was joined to the pumping and the gas-filling side of the apparatus. (The position of the reaction flask E is shown in the figure during the filling procedure.) All quick-fits shown are standard B7 or B10 tapers.

The thermostated silicone oil-bath consisted of a

four liter glass beaker insulated by polystyrene foam on all sides and enclosed by a wooden box with a small circular hole for the observation of the colour changes of the reaction mixture. A perspex rectangular tank was used as the thermostated water-bath. A "Jumo" thermo regulator with a "merc to merc" relay control circuit, and heating provided by a 25 watt elongated light bulb were used for the operation of both thermostat units. The temperatures could be maintained within $\pm 0.05^\circ$ using mechanical stirring and good insulation.

(D) Procedure

The following describes the technique used for a typical hydrogen uptake measurement experiment. The system was found to be extremely sensitive to trace amounts of oxygen; therefore oxygen-free conditions were ensured while preparing the reaction mixture (solution of $\text{Ir}(\text{CO})\text{X}(\text{PPh}_3)_2$ and substrate in DMA) by maintaining a continuous flow of nitrogen through the reaction flask. The solid reactants were weighed out in glass capsules which were then placed in the reaction flask. The reaction flask was then connected to the glass spiral at A and the spiral was attached to the apparatus at C through the tap D. The other neck B of the reaction flask was closed by the tap F. The nitrogen gas

source was connected by rubber tubing (previously flushed with nitrogen) through the tap Y to the apparatus at N. The gas was pumped off from the whole system including the spiral and the reaction flask up to tap Y by opening taps T, C, D, H, I, J and S and the needle valve G. The needle valve was then closed and nitrogen was admitted by opening the tap Y followed by the slow opening of the needle valve to allow gas into the whole system up to tap T. When the pressure (read from the manometer R) reached slightly above one atmosphere, the tap F was opened and a continuous nitrogen stream was maintained through the system. Nitrogen was separately bubbled through dimethylacetamide (DMA) for about 45 minutes, and 5 mls of this oxygen-free DMA were pipetted (the pipette was preflushed with nitrogen) into the reaction flask at B after removing the tap F while the flow of nitrogen gas through the system was maintained. The end B of the reaction flask was closed with a B7 stopper and the needle valve and the tap Y were closed to stop the nitrogen flow. Nitrogen was then pumped off thoroughly from the system to the right of the needle valve and hydrogen gas was admitted through the tap W to a convenient pressure. The taps C and D were then closed and the spiral along with the reaction vessel was moved and attached at N and X, the reaction flask being placed in the oil-bath. The rest of the system beyond D was then evacuated and filled with

hydrogen to a convenient pressure. The tap D was then opened and the pressure in the system adjusted to the required reaction pressure. The shaker was then started, the taps I and J were closed and the timer started.

The gas uptake was indicated by the change of the oil levels in the capillary manometer M. At appropriate time intervals more hydrogen was admitted into the gas-burette by opening the needle valve slowly to bring the oil levels in the manometer M in line. The pressure in the reaction flask was thus kept constant during the course of the reaction. The consequent changes in the mercury level L in the gas-burette were measured using a vertically mounted travelling telescope. The volume of the hydrogen taken up was calculated from the diameter of the tube L and a plot of hydrogen uptake (in moles per liter) versus time could be drawn.

The occurrence of diffusion controlled processes was avoided by using small volumes of the solution in a reaction flask with an indented surface and maintaining a rapid shaking rate.

(E) Spectrophotometric Measurements

The kinetics and equilibria of a number of reactions have been studied using spectrophotometric techniques in the visible/UV range. A specially constructed silica cell with an optical path length of 5 cms was used and is shown in

figure 4. Oxygen-free conditions were also required in these experiments. The technique used to obtain such conditions was similar to that used in hydrogen uptake measurement experiments. The reactants were weighed in small glass capsules which were then placed in the reaction cell. The presence of capsules did not interfere with the passage of the light beam through the cell. The reaction cell was attached to the spiral, at A' in place of the reaction flask as shown in figure 3, and the operations leading to a steady stream of nitrogen gas through the cell were carried out. Eleven mls of oxygen-free dimethylacetamide were then pipetted into the reaction cell through B' while the nitrogen flow was maintained. The outlet B' was then closed with a B7 stopper and the gas stream stopped. The tap Z was closed, and the reaction cell was detached from the spiral and then shaken to dissolve the reactants. Using similar procedures the cell could, if necessary, be filled with other gaseous atmospheres such as hydrogen.

Optical density measurements were made on a Cary 14 Recording Spectrophotometer fitted with a constant temperature water circulator which could be operated from ambient temperatures up to 80°C. Reaction rates could be investigated by following the disappearance of selected absorption peaks with time.

Reflection spectra of powdered samples were measured

over the range 750-320 μ with a Bausch and Lomb Spectronic 600 Spectrophotometer fitted with a diffuse reflection attachment and a magnesium carbonate reference disc. Infrared spectra were taken with a Perkin-Elmer Model 21 Spectrophotometer using KBr discs.

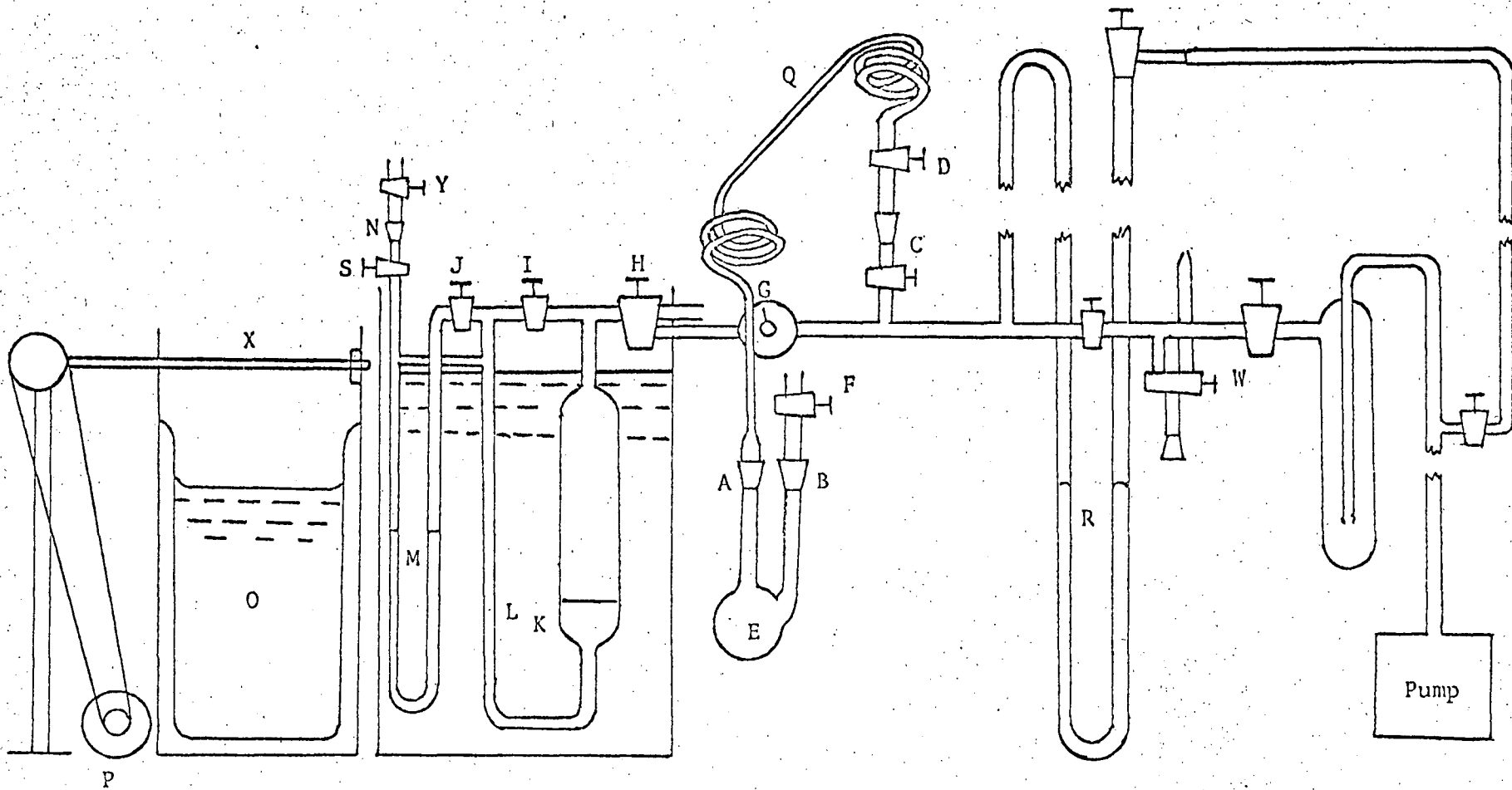


FIGURE 3. THE HYDROGENATION APPARATUS

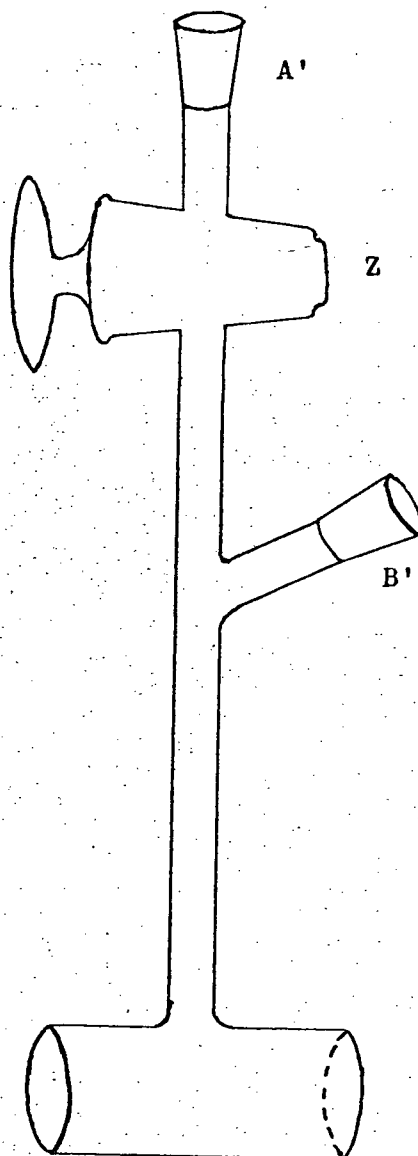


FIGURE 4
REACTION CELL FOR SPECTROPHOTOMETRIC STUDIES.

III. RESULTS OF GAS UPTAKE MEASUREMENTS

1. Ir(CO)Cl(PPh₃)₂ Systems

Figure 5 shows a typical gas uptake plot for the hydrogenation of maleic acid catalysed by the Ir(CO)Cl(PPh₃)₂ complex in dimethylacetamide at 80°; in the absence of the iridium complex there was no measurable uptake. The curve initially shows slight antocatalysis, the rate then becoming linear and finally falling to zero at the complete reduction of the maleic acid. The succinic acid had previously been isolated by sublimation³⁹ and had been identified by infrared spectrum and melting point. The system was extremely sensitive to the presence of traces of oxygen and a variety of improvements in the experimental technique was necessary before reasonably consistent results were obtained. The rates in the linear region have been estimated from the uptake plots for series of experiments.

The variation in the linear rate with the iridium concentration for the chloro complex is shown in Table I and shown graphically in figures 6 and 7. The dependence is seen to be between zero and first order being essentially first order at lower iridium concentration and tending to become zero order at the higher iridium concentration when the rate approaches a limiting value.

The results obtained for similar sets of experiments in which the reaction solution had been left under nitrogen overnight at 80° (Table II and figure 7) or at room temperature for ten days (Table III) prior to hydrogenation show a similar dependence on iridium concentration but the rates are roughly 1.5 and 2.5 times greater than those listed in Table I, where immediate hydrogenation was carried out.

The results of the variation of maleic acid concentration are given in Table IV and are shown graphically in figure 8. Again a dependence between zero and first order is observed with the rate approaching a limiting value at the highest maleic acid concentration used.

Table V lists data for the variation of rate with the hydrogen pressure and the plot in figure 9 demonstrates between zero and first order dependence as obtained for the iridium and maleic acid dependences. Table VI gives data for a similar series of experiments at twice the iridium concentration for solutions which had been left at room temperature for ten days prior to hydrogenation and again it is seen that a limiting rate is being approached with increasing hydrogen pressure.

Table VII shows the effect of addition of 10^{-2} M LiCl, LiNO₃ and triphenylphosphine on the hydrogenation rate of a typical experiment. Chloride inhibits the reaction by a factor of about 3 and the nitrate addition shows that this inhibition is not due to salt effects. The added

TABLE I

Variation of $\text{Ir}(\text{CO})\text{Cl}(\text{PPh}_3)_2$ concentration in the hydrogenation of maleic acid (7.0×10^{-2} M) in DMA at 80° and 730 mm hydrogen pressure

Concentration of $\text{Ir}(\text{CO})\text{Cl}(\text{PPh}_3)_2$ $\times 10^3$ M	5.36	2.68	1.34	0.67
Linear Rate $\times 10^6$ $\text{M}^{-1} \text{s}^{-1}$	3.81	2.92	(a) 1.97	1.24
	4.0		(b) 2.50	

TABLE II

Variation of $\text{Ir}(\text{CO})\text{Cl}(\text{PPh}_3)_2$ concentration in the hydrogenation of maleic acid at 80° and 730 mm pressure of hydrogen; using stock solution of 5.36×10^{-3} M $\text{Ir}(\text{CO})\text{Cl}(\text{PPh}_3)_2$ and 7.0×10^{-2} M maleic acid in DMA left overnight at 80° under nitrogen before hydrogenation

Concentration of $\text{Ir}(\text{CO})\text{Cl}(\text{PPh}_3)_2$ $\times 10^3$ M	5.36	3.20	2.14	1.07
Linear Rate $\times 10^6$ $\text{M}^{-1} \text{s}^{-1}$	5.51	4.9	4.73	3.54

TABLE III

Variation of $\text{Ir}(\text{CO})\text{Cl}(\text{PPh}_3)_2$ concentration in the hydrogenation of maleic acid at 80° and 730 mm pressure of hydrogen; using stock solution of 5.36×10^{-3} M $\text{Ir}(\text{CO})\text{Cl}(\text{PPh}_3)_2$ and 7.0×10^{-2} M maleic acid in DMA left for ten days at room temperature under nitrogen before hydrogenation

Concentration of $\text{Ir}(\text{CO})\text{Cl}(\text{PPh}_3)_2$ $\times 10^3$ M	5.36	2.68	1.34
Linear Rate $\times 10^6$ $\text{M}^{-1} \text{s}^{-1}$	9.2	7.2	4.57

TABLE IV

Variation of maleic acid concentration in the hydrogenation of maleic acid using 5.36×10^{-3} M $\text{Ir}(\text{CO})\text{Cl}(\text{PPh}_3)_2$ in DMA at 80° and 730 mm pressure of hydrogen

Concentration of Maleic acid $\times 10^2$ M	7.0	3.5	2	1
Linear Rate $\times 10^6$ $\text{M}^{-1} \text{s}^{-1}$	3.7	2.52	2.4	1.7

TABLE V

Variation of hydrogen pressure in the hydrogenation of maleic acid (7.0×10^{-2} M) using 1.34×10^{-3} M $\text{Ir}(\text{CO})\text{Cl}(\text{PPh}_3)_2$ in DMA at 80°

Hydrogen Pressure in mm Hg	730	365	175
Linear Rate	(a) 1.97	(a) 1.34	(a) 1.11
$\times 10^6 \text{ M}^{-1} \text{ s}^{-1}$	(b) 2.50	(b) 1.57	(b) 1.05

TABLE VI

Variation of hydrogen pressure in the hydrogenation of maleic acid in DMA at 80° using the same stock solution as for experiments listed in Table III

Concentration of $\text{Ir}(\text{CO})\text{Cl}(\text{PPh}_3)_2$ 2.68×10^{-3} M
 Concentration of maleic acid 7.0×10^{-2} M

Hydrogen Pressure in mm Hg	730	365	180
Linear Rate			
$\times 10^6 \text{ M}^{-1} \text{ s}^{-1}$	7.2	5.95	5.06

TABLE VII

Hydrogenation of 7.0×10^{-2} M maleic acid in DMA using 5.36×10^{-3} M $\text{Ir}(\text{CO})\text{Cl}(\text{PPh}_3)_2$ at 80° and 730 mm pressure of hydrogen. Effect of adding various reagents at a concentration of 10^{-2} M

Added Compound		No additive	LiCl	LiNO_3	$(\text{C}_6\text{H}_5)_3\text{P}$
Rate	initial	1.9	0.7	--	~0.2
$\times 10^6 \text{ M}^{-1} \text{ s}^{-1}$	linear	3.62	--	3.62	--

TABLE VIII

Variation of $\text{Ir}(\text{CO})\text{Cl}(\text{PPh}_3)_2$ concentration in the hydrogenation of fumaric acid (7.0×10^{-2} M) in DMA at 80° and 730 mm hydrogen pressure

Concentration of $\text{Ir}(\text{CO})\text{Cl}(\text{PPh}_3)_2$ $\times 10^3 \text{ M}$	8.04	5.36	2.68
Linear Rate $\times 10^7 \text{ M}^{-1} \text{ s}^{-1}$	7.5	4.0	4.0

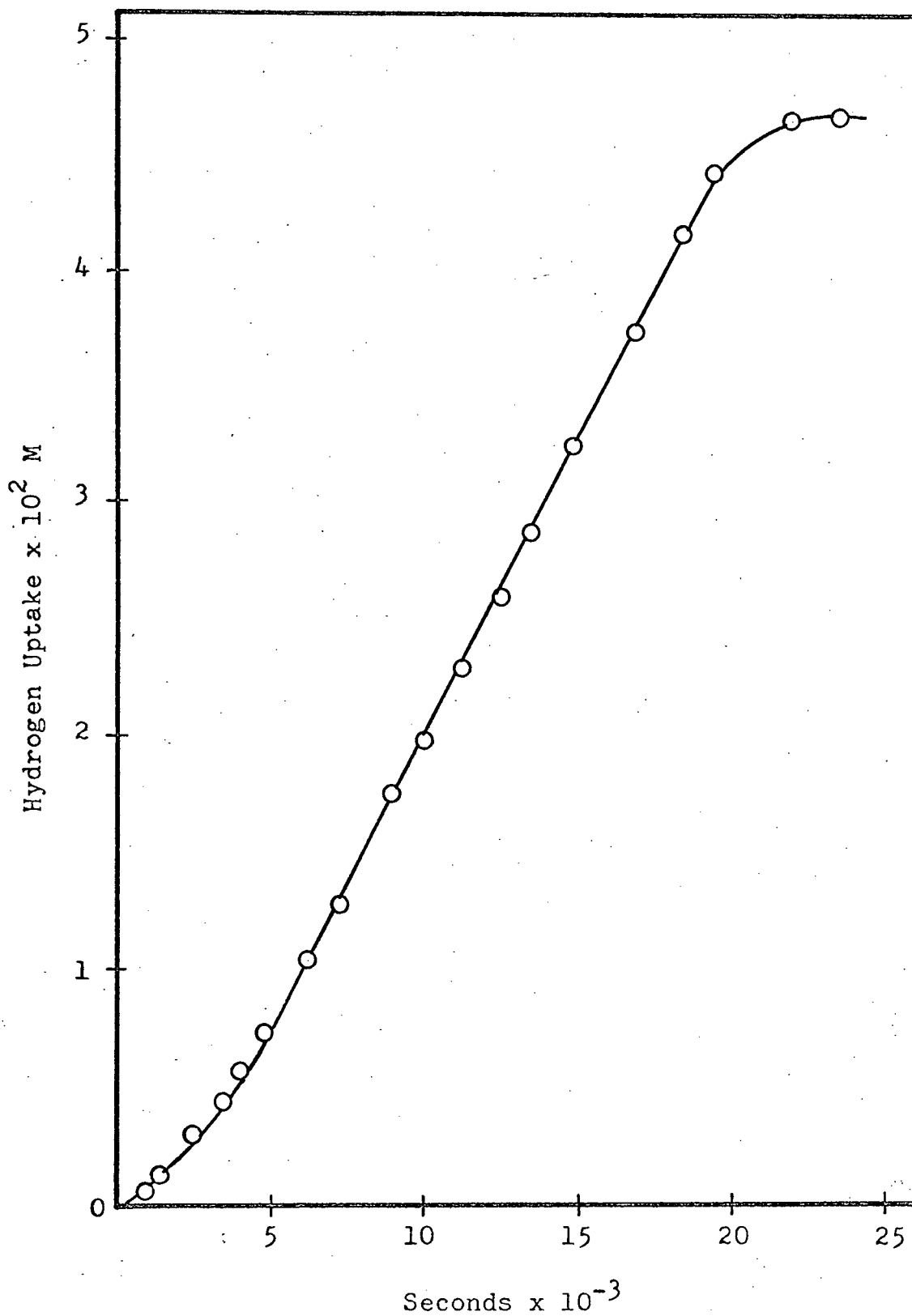


Figure 5: A Typical Hydrogen Uptake Plot
[Ir(CO)Cl(PPh₃)₂] = 5.38×10^{-3} M
[Maleic acid] = 3.5×10^{-2} M
Temperature 80° and hydrogen pressure 730. mm

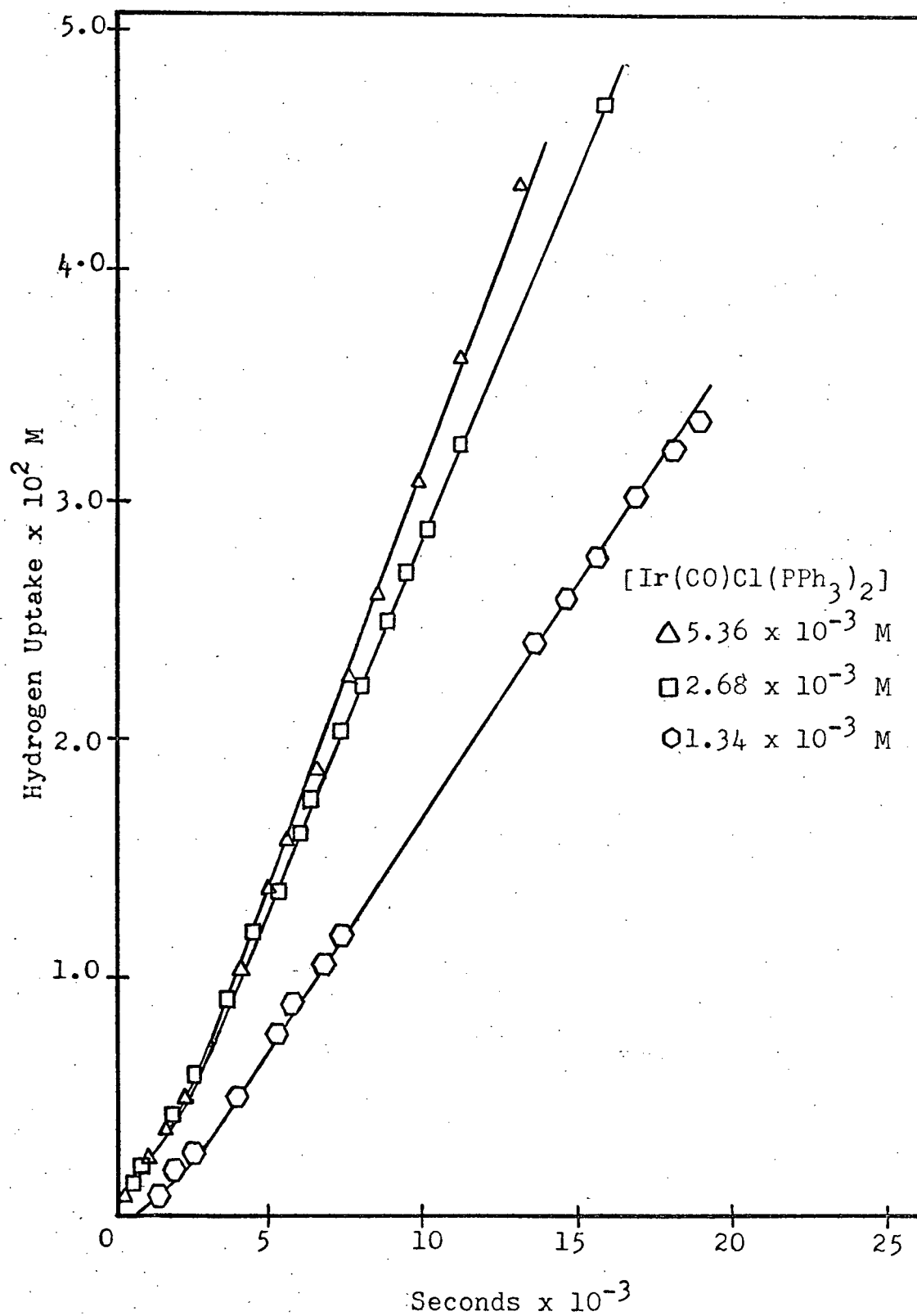


Figure 6: Effect of the Variation of $\text{Ir(CO)Cl(PPh}_3)_2$ conc. on the Uptake Plots (see Table I)

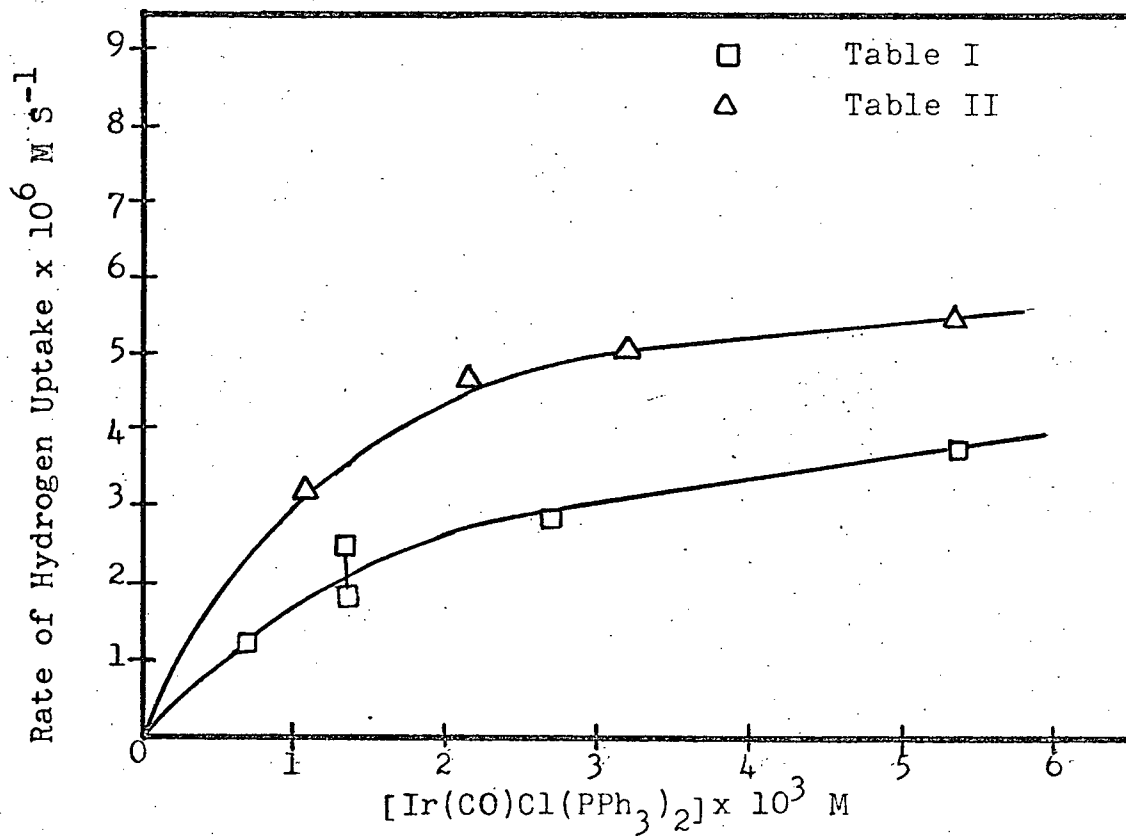


Figure 7: Variation of rate with $\text{Ir}(\text{CO})\text{Cl}(\text{PPh}_3)_2$ Concentration

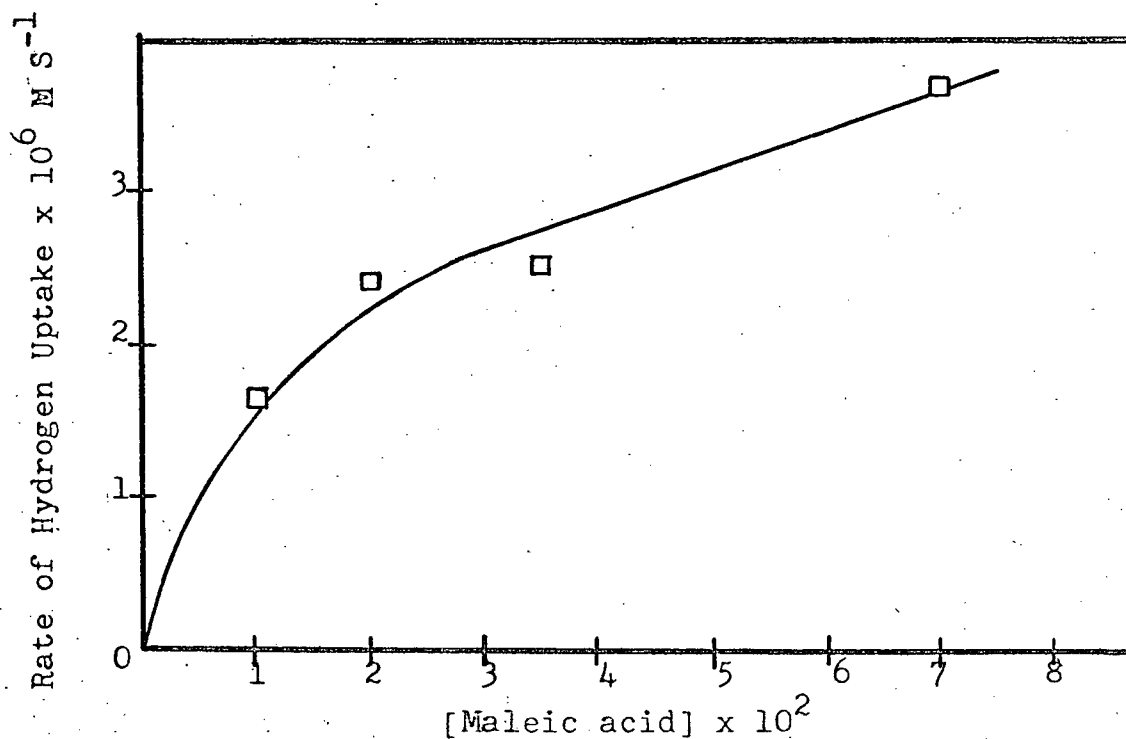


Figure 8: Variation of rate with maleic acid Concentration (see Table IV)

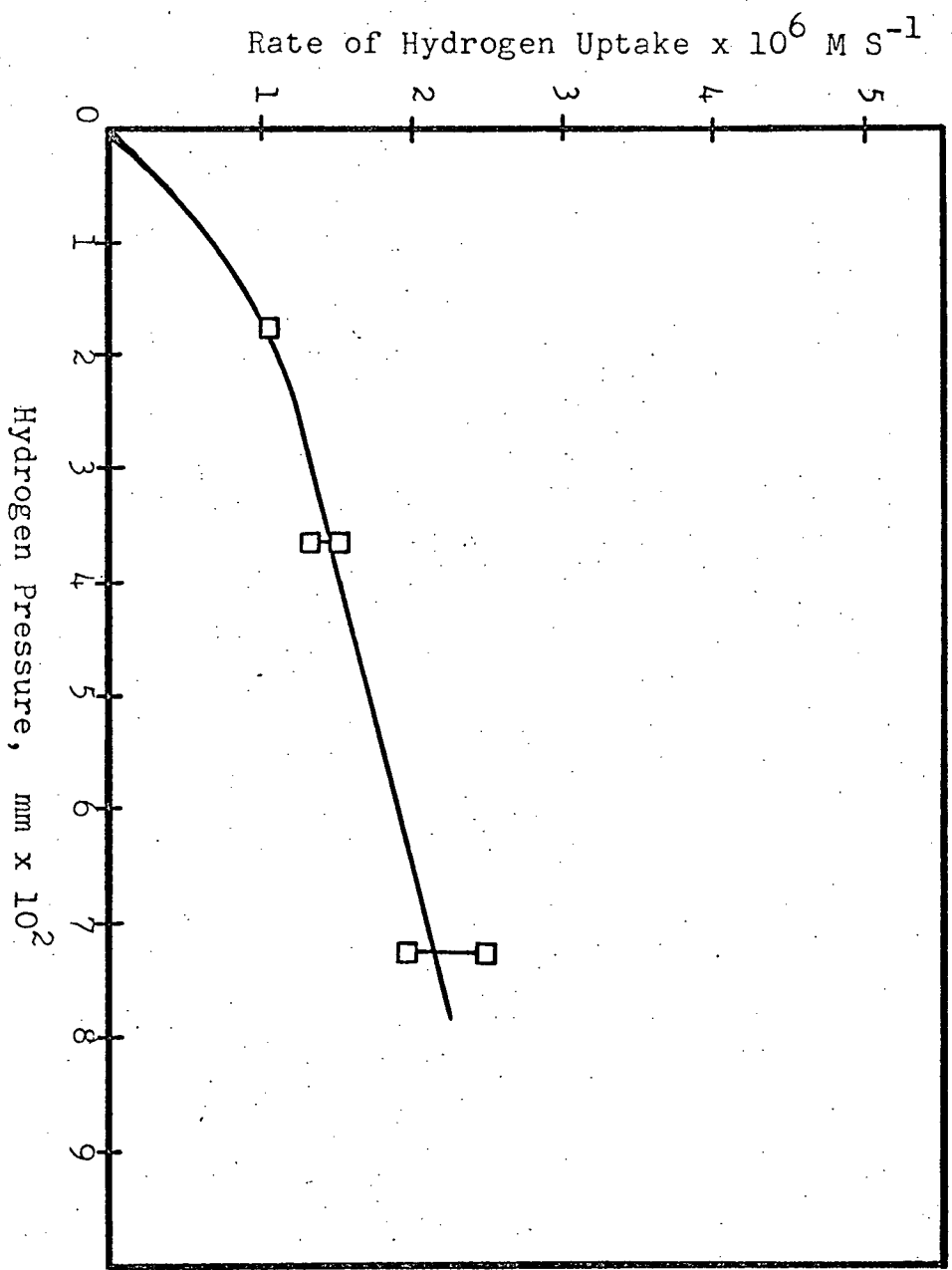


Figure 9: Variation of rate with hydrogen pressure (see Table V)

triphenylphosphine practically stops the hydrogenation altogether.

Much slower reactions were observed when fumaric acid was used as substrate (Table VIII). The uptake plots were similar to those for maleic acid as substrate but the rates fell off more rapidly and the linear region was not so clearly pronounced (see figure 10); the rates were roughly 7 to 8 times slower than those for corresponding maleic acid systems.

Uptake plots using dimethylsulphoxide as solvent were very similar to those observed in the dimethylacetamide system although the initial autocatalysis region was more pronounced than in the latter. An extended linear region was again observed where the rates were about half those of the corresponding reactions in dimethylacetamide solution (Table IX). The initial rates were about three times slower in the dimethylsulphoxide system.

2. $\text{Ir}(\text{CO})\text{Br}(\text{PPh}_3)_2$ Systems

Hydrogen uptake plots for the hydrogenation of maleic acid using the bromo complex were very similar to those obtained in the case of chloro complex although the initial autocatalysis reaction was less pronounced. The results of the variation of the concentration of $\text{Ir}(\text{CO})\text{Br}(\text{PPh}_3)_2$ are given in Table X. The rates of the reaction in the linear region were about 2.5 times greater than those obtained for chloro complex. The dependence of the linear rate is again

seen to be between zero and first order, approaching a limiting value at higher concentrations of $\text{Ir}(\text{CO})\text{Br}(\text{PPh}_3)_2$.

The variation in rate with maleic acid concentration for the bromo complex (in 2 experiments) is given in Table XI. The data for the hydrogen pressure variation listed in Table XII show that the rate dependence is between zero and first order as obtained in the case of chloro complex.

3. $\text{Ir}(\text{CO})\text{I}(\text{PPh}_3)_2$ Systems

Table XIII lists the variation of the linear rate with $\text{Ir}(\text{CO})\text{I}(\text{PPh}_3)_2$ concentration and shows a first order dependence of rate on the iridium concentration. The rates are about four times greater than those obtained for the corresponding chloro complex reactions.

The variation of rate with the maleic acid concentration is given in Table XIV and the variation of hydrogen pressure is listed in Table XV; again between zero and first order is indicated for these reactions.

4. Ethylene as Substrate

No measurable gas uptake was observed for three hours when hydrogenation of ethylene (365 mm Hg of C_2H_4 , 400 mm Hg of H_2) was attempted in benzene at temperatures up to 55° using 5.0×10^{-3} M $\text{Ir}(\text{CO})\text{Cl}(\text{PPh}_3)_2$. Very slow gas uptake was, however, observed when DMA was used instead of benzene

TABLE IX

Variation of $\text{Ir}(\text{CO})\text{Cl}(\text{PPh}_3)_2$ concentration in the hydrogenation of maleic acid (7.0×10^{-2} M) in DMSO at 80° and 730 mm hydrogen pressure

Concentration of $\text{Ir}(\text{CO})\text{Cl}(\text{PPh}_3)_2$ $\times 10^3$ M	5.36	2.68
Linear Rate $\times 10^6$ $\text{M}^{-1} \text{s}^{-1}$	1.69	1.30

TABLE X

Variation of $\text{Ir}(\text{CO})\text{Br}(\text{PPh}_3)_2$ concentration in the hydrogenation of 7.0×10^{-2} M maleic acid in DMA at 80° and 730 mm pressure of hydrogen

Concentration of $\text{Ir}(\text{CO})\text{Br}(\text{PPh}_3)_2$ $\times 10^3$ M	5.06	2.53	1.266
Linear Rate $\times 10^6$ $\text{M}^{-1} \text{s}^{-1}$	8.27	5.91	4.73

TABLE XI

Variation of maleic acid concentration in the hydrogenation using 5.06×10^{-3} M $\text{Ir}(\text{CO})\text{Br}(\text{PPh}_3)_2$ in DMA at 80° and 730 mm hydrogen pressure

Concentration of maleic acid $\times 10^2$ M	7.0	3.5
Linear Rate $\times 10^6$ $\text{M}^{-1} \text{S}^{-1}$	8.27	~ 10.4

TABLE XII

Hydrogen pressure variation in the hydrogenation of 7.0×10^{-2} M maleic acid using 2.53×10^{-3} M $\text{Ir}(\text{CO})\text{Br}(\text{PPh}_3)_2$ in DMA at 80°

Hydrogen pressure in mm Hg	730	365	184
Linear Rate $\times 10^6$ $\text{M}^{-1} \text{S}^{-1}$	5.91	3.77	2.36

TABLE XIII

Variation of $\text{Ir}(\text{CO})\text{I}(\text{PPh}_3)_2$ concentration in the hydrogenation of 7.0×10^{-2} M maleic acid in DMA at 80° and 730 mm hydrogen pressure

Concentration of $\text{Ir}(\text{CO})\text{I}(\text{PPh}_3)_2$ $\times 10^3$ M	2.68	1.34	0.67
Linear Rate $\times 10^6$ $\text{M}^{-1} \text{S}^{-1}$	13.4	6.38	2.91

TABLE XIV

Variation of maleic acid concentration in the hydrogenation using 2.68×10^{-3} M $\text{Ir}(\text{CO})\text{I}(\text{PPh}_3)_2$ in DMA at 80° and 730 mm hydrogen pressure

Maleic acid concentration $\times 10^2$ M	7.0	3.5
Linear Rate $\times 10^6$ $\text{M}^{-1} \text{S}^{-1}$	13.4	10.5

TABLE XV

Variation of hydrogen pressure in the hydrogenation of 7.0×10^{-2} M maleic acid using 2.01×10^{-3} M $\text{Ir}(\text{CO})\text{I}(\text{PPh}_3)_2$ in DMA at 80° (the iodo complex had decomposed)

Hydrogen pressure in mm Hg	730	365
Linear Rate $\times 10^6 \text{ M}^{-1} \text{ S}^{-1}$	4.88	3.65

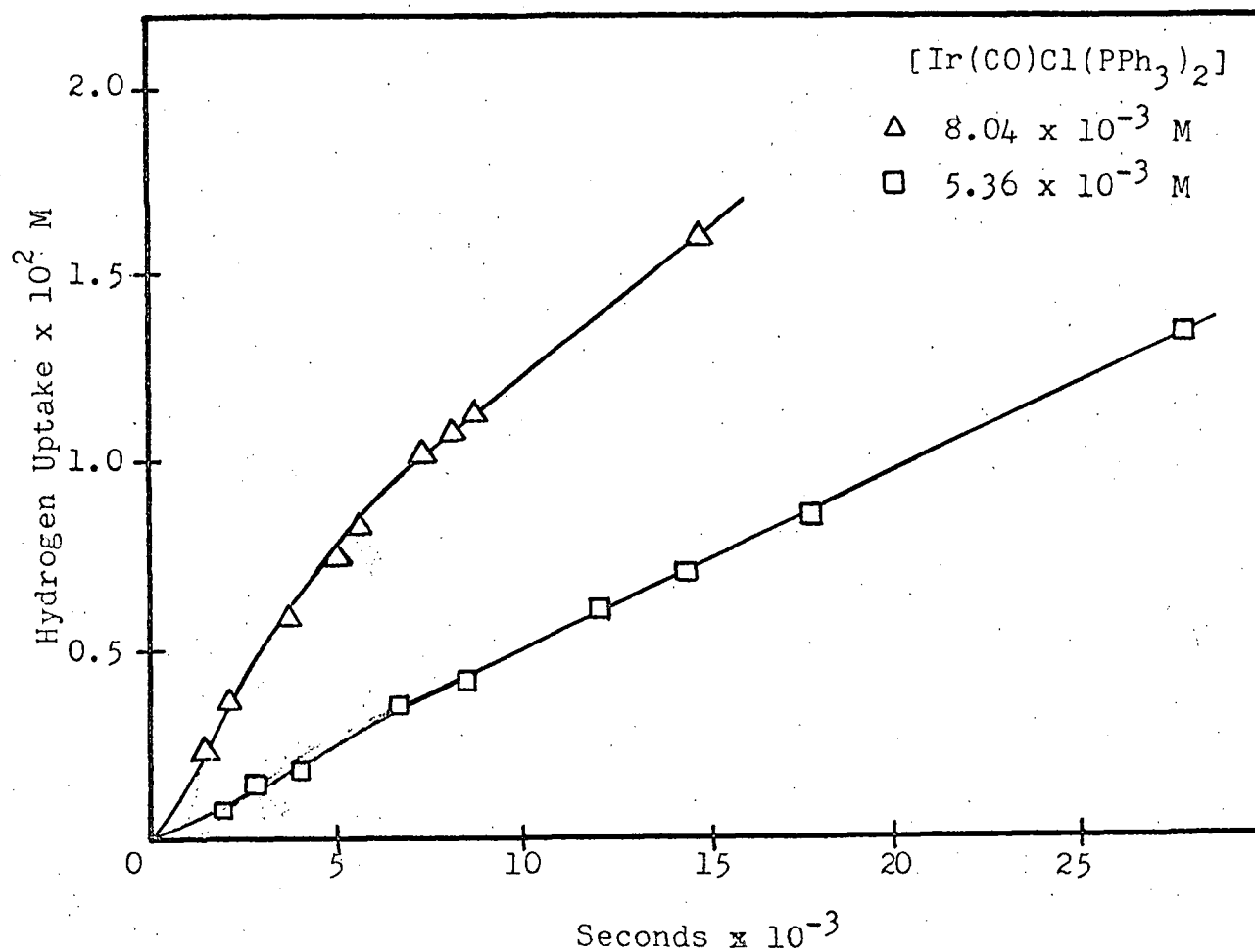


Figure 10: Effect of Variation of Ir(CO)Cl(PPh₃)₂ Concentration on Uptake Plots when fumaric acid is used as Substrate (see Table VIII)

as the solvent at 80° under otherwise identical conditions. In ten hours the uptake was about 1.6×10^{-2} moles per liter.

5. Effect of Oxygen on rates of hydrogenation

Earlier work in this laboratory³⁹ had shown that small amounts of molecular oxygen present in the $\text{Ir}(\text{CO})\text{Cl}(\text{PPh}_3)_2$ --maleic acid--hydrogen system enhanced the rates of hydrogenation considerably; a few per cent of added oxygen in the gas phase had increased rates by a factor of about a hundred. This effect of oxygen was soon confirmed, and the experimental technique for "oxygen free" conditions was considered sufficient when reproducible minimum hydrogenation rates were attained. The somewhat enhanced rates given in Tables II, III and VI for solutions that had been left under nitrogen prior to hydrogenation are presumably due to traces of oxygen present in the system.

IV. SPECTROPHOTOMETRIC RESULTS

The gas uptake measurements clearly indicated that the hydrogenation reactions are not simple. Independent spectrophotometric studies were carried out to investigate separately the equilibrium between the iridium chloro complex and molecular hydrogen (equation 1) and the possibility of reaction between the chloro complex and maleic acid substrate. This chapter summarizes the results of these studies. The characteristic spectrum exhibited by the chloro complex is shown in figure 11 (λ_{\max} : 340 m μ , $\epsilon = 2.8 \times 10^3$; λ_{\max} : 387 m μ , $\epsilon = 3.4 \times 10^3$; λ_{\max} : 339 m μ , $\epsilon = 7.0 \times 10^2$).

1. Ir(CO)Cl(PPh₃)₂/H₂ Equilibrium

At the temperature above 30^o, Ir(CO)Cl(PPh₃)₂ in DMA solution undergoes a rapid reversible reaction with hydrogen as a result of which the yellow colour of the complex fades considerably. The reaction was studied by following the optical density changes at 387 m μ (the dihydride complex absorbs only slightly at this wave length, $\epsilon \approx 500$). At room temperature and 730 mm hydrogen pressure the dihydride complex is essentially fully formed:



More extensive data for this system have been obtained earlier

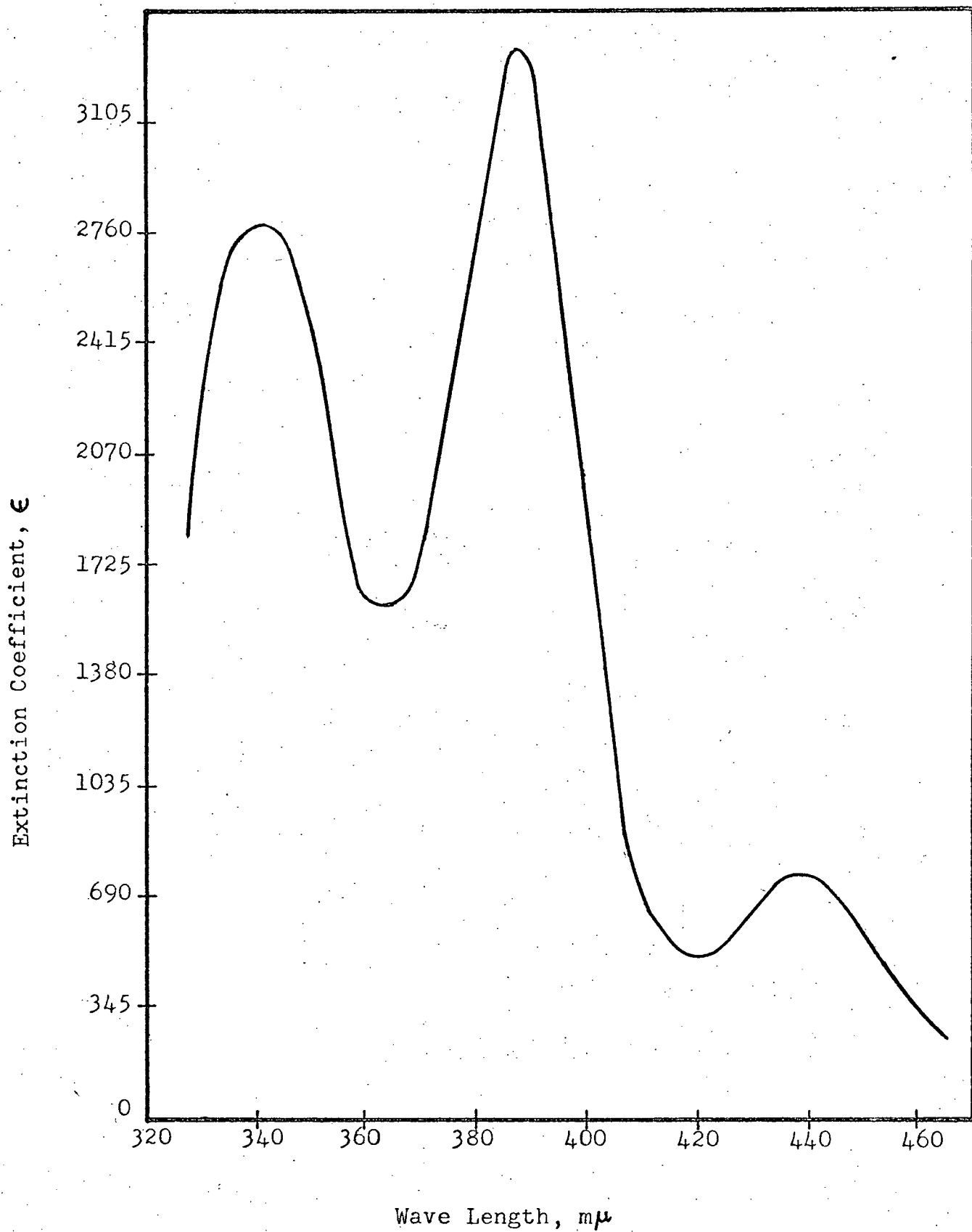


Figure 11. Spectrum of $\text{Ir}(\text{CO})\text{Cl}(\text{PPh}_3)_2$ (1.16×10^{-4} M) in DMA; path length 5 cms.

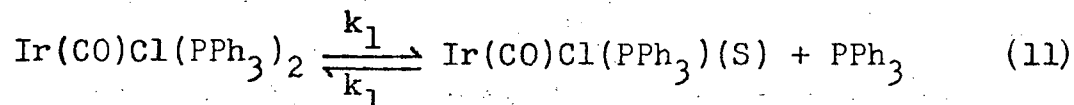
in this laboratory by James and McLaughlin.³⁹ Their results from spectrophotometric studies are shown below:

Temperature	40°	50°	60°	70°	80°
K_H^r	5.3	2.4	1.7	1.0	0.6

where $K_H^r = K_H[H_2]$.

2. Ir(CO)Cl(PPh₃)₂ Solutions without Substrates

In benzene solution the spectrum of the chloro complex does not change with time provided the solution was made under oxygen-free conditions and kept under nitrogen. In DMA solutions, however, the optical density decreased slowly and this change in optical density (at 387 μ) was followed as a function of time. The plots of optical density against time at 25° and 80° are shown in figure 12. No change in optical density was observed when excess triphenylphosphine (10^{-2} M) was added to the DMA solution. Conductivity measurements indicate that chloride is not being formed by dissociation of the complex and there was no evolution of gas when a solution of the chloro complex was shaken overnight at 80° under nitrogen indicating that the carbonyl group does not come off as gaseous carbon monoxide. All this evidence leads to the conclusion that the dissociation reaction



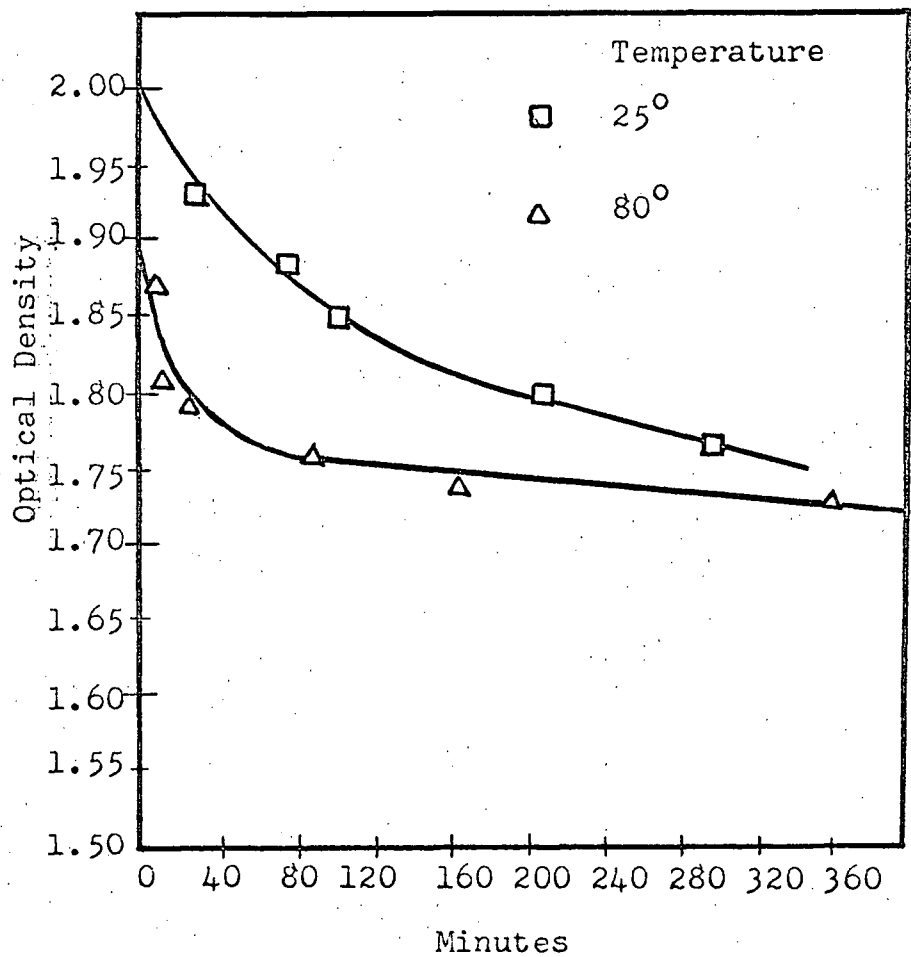


Figure 12: Plots of O.D. against time for $\text{Ir}(\text{CO})\text{Cl}(\text{PPh}_3)_2$ (1.16×10^{-4} M) in DMA in the absence of any substrate (Blank)

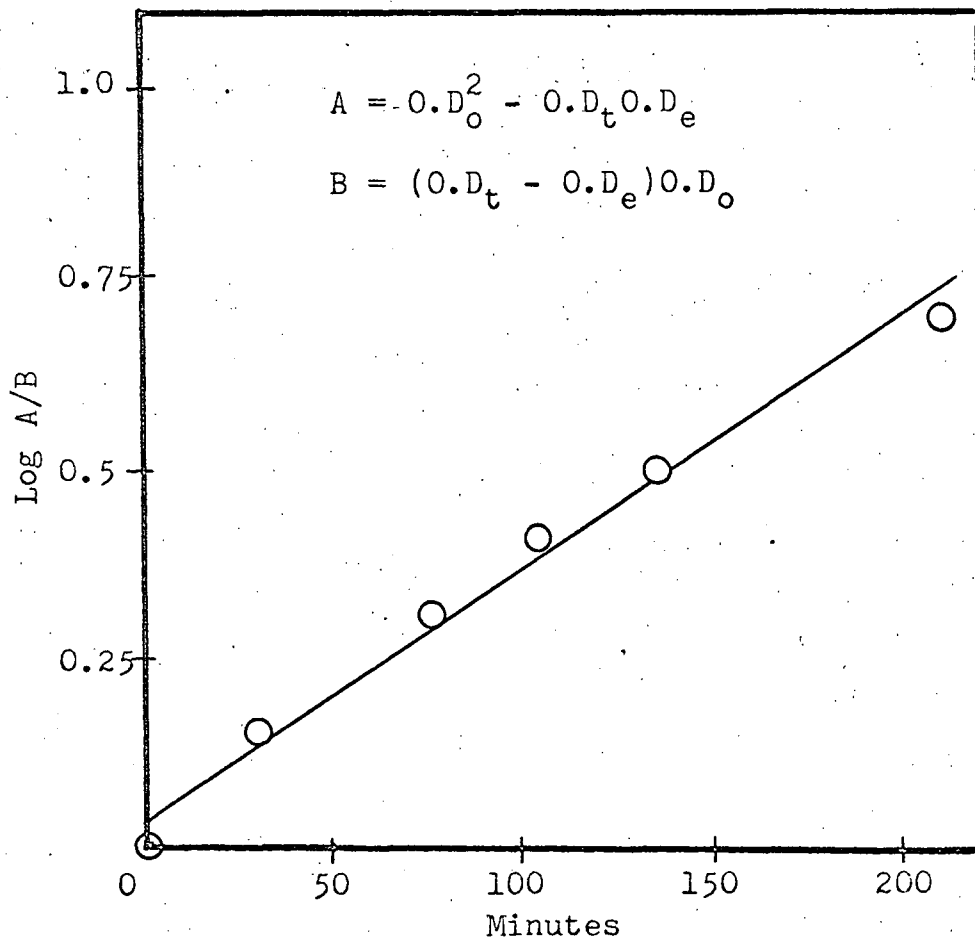


Figure 13: Plot of $\log A/B$ against time for the "Blank" reaction at 25° (see figure 12)

is occurring in DMA solution, a solvent molecule (S) presumably coordinating. This process can be analysed by standard procedures⁴⁰ by the relationship

$$\log \frac{O.D_o^2 - O.D_t O.D_e}{(O.D_t - O.D_e)O.D_o} = \frac{k_1}{2.3(O.D_o - O.D_e)} t \quad (12)$$

where $O.D_o$ = initial optical density of the $\text{Ir}(\text{CO})\text{Cl}(\text{PPh}_3)_2$ complex

$O.D_t$ = optical density at time t of the $\text{Ir}(\text{CO})\text{Cl}(\text{PPh}_3)_2$ complex

$O.D_e$ = optical density at equilibrium of the $\text{Ir}(\text{CO})\text{Cl}(\text{PPh}_3)_2$ complex.

The slope of a plot of $\log \frac{O.D_o^2 - O.D_t O.D_e}{(O.D_t - O.D_e)O.D_o}$ against time

gives k_1' ($k_1' = \frac{k_1}{2.3(O.D_o - O.D_e)}$). Such a plot for the data

at 25° is shown in figure 13 and is reasonably linear.

Absorption of the $\text{Ir}(\text{CO})\text{Cl}(\text{PPh}_3)(\text{S})$ species at $387 \text{ m}\mu$ was taken as zero; the slight curvature results from a small contribution to the absorption by this species. The slope of the plot gives $k_1 = 10^{-5} \text{ Sec}^{-1}$. The equilibrium constant for the reaction is readily calculated from the initial and final optical densities:

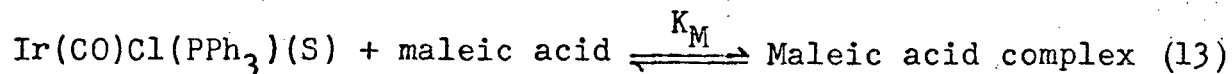
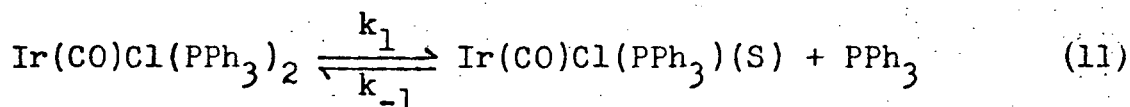
$$K = \frac{[\text{Ir}(\text{CO})\text{Cl}(\text{PPh}_3)(\text{S})][\text{P}]}{[\text{Ir}(\text{CO})\text{Cl}(\text{PPh}_3)_2]} = 2.6 \times 10^{-6} \text{ M}$$

and since $K = k_1/k_{-1}$, $k_{-1} = 3.9 \text{ M}^{-1} \text{ Sec}^{-1}$.

A similar treatment of the optical density data at 80° gives the approximate values $k_1 \sim 10^{-4} \text{ Sec}^{-1}$, $k_{-1} \sim 75 \text{ M}^{-1} \text{ Sec}^{-1}$, $K \sim 1.3 \times 10^{-6} \text{ M}$; the plot to give k_1 is considerably more curved than that for the data at 25° and the value of 10^{-4} Sec^{-1} is computed from an initial linear slope.

3. Complexing with maleic acid

In the presence of maleic acid the decrease in the optical density for $\text{Ir}(\text{CO})\text{Cl}(\text{PPh}_3)_2$ in DMA is much greater than in a corresponding "blank" in the absence of maleic acid. Some plots of optical density against time obtained for the $\text{Ir}(\text{CO})\text{Cl}(\text{PPh}_3)_2$ /maleic acid/DMA system at different conditions are shown in figure 14. No change in optical density was observed for these systems when 10^{-2} M triphenylphosphine was added to the solutions, indicating that triphenylphosphine which inhibits the dissociation reaction of $\text{Ir}(\text{CO})\text{Cl}(\text{PPh}_3)_2$ (equation 11) also inhibits the complex formation with maleic acid. This suggests that the maleic acid forms the complex with the solvated species, $\text{Ir}(\text{CO})\text{Cl}(\text{PPh}_3)(\text{S})$ rather than with the original complex, $\text{Ir}(\text{CO})\text{Cl}(\text{PPh}_3)_2$:



If the second step is a relatively fast equilibrium, the sys-

tem may be analysed in the following way:

The rate equation for the first step is

$$-\frac{dA}{dt} = k_1 A - k_{-1} BC \quad (14)$$

where $A = [\text{Ir}(\text{CO})\text{Cl}(\text{PPh}_3)_2]$, $B = [\text{Ir}(\text{CO})\text{Cl}(\text{PPh}_3)(\text{S})]$, and $C = [\text{PPh}_3]$, and the second step gives

$$K_M = \frac{D}{B[\text{M.A}]}$$

where $D = [\text{Maleic acid complex}]$ and $\text{M.A} = \text{maleic acid}$.

Since

$$B_0 = C_0 = 0 \text{ (initial concentrations)}$$

$$\text{therefore, } C = B + D \text{ or } C = B(1 + K_M[\text{M.A}]) \quad (15)$$

The initial concentration $A_0 = A + C$

Substituting from 15

$$A_0 = A + B(1 + K_M[\text{M.A}])$$

$$\text{therefore, } B = \frac{A_0 - A}{1 + K_M[\text{M.A}]} \quad \text{and}$$

$$BC = \frac{(A_0 - A)^2}{1 + K_M[\text{M.A}]}$$

Substituting for BC in equation 14

$$-\frac{dA}{dt} = k_1 A - k_{-1} \frac{(A_0 - A)^2}{1 + K_M[\text{M.A}]} \quad (16)$$

which at equilibrium becomes

$$k_1 A_e = k_{-1} \frac{(A_0 - A_e)^2}{1 + K_M[\text{M.A}]}, \text{ where } A_e \text{ is the equilibrium concentration.}$$

$$\text{i.e. } k_{-1} = k_1 \frac{A_e}{(A_o - A_e)^2} (1 + K_M[M.A])$$

Substitution for k_{-1} in equation 16 gives

$$\begin{aligned} -\frac{dA}{dt} &= k_1 A - \frac{k_1 A_e (1 + K_M[M.A])}{(A_o - A_e)^2} \frac{(A_o - A)^2}{1 + K_M[M.A]} \\ &= k_1 \left[A - \frac{A_e}{(A_o - A_e)^2} (A_o - A)^2 \right] \end{aligned} \quad (17)$$

The integration of 17 gives

$$\log \frac{A_o^2 - A_e A}{(A - A_e) A_o} = \frac{k_1}{2.3} \left(\frac{A_o + A_e}{A_o - A_e} \right) t$$

which can be written in the form of optical densities (O.D.):

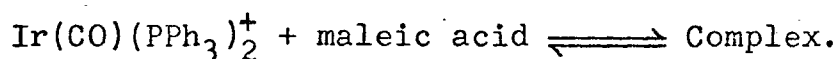
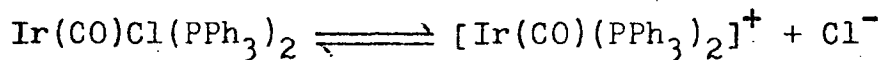
$$\log \frac{O.D_o^2 - O.D_t O.D_e}{(O.D_t - O.D_e) O.D_o} = \frac{k_1}{2.3} \left(\frac{O.D_o + O.D_e}{O.D_o - O.D_e} \right) t \quad (18)$$

The result is the same expression as that obtained for the dissociation reaction (11) on its own.

The plots of $\log \frac{O.D_o^2 - O.D_t O.D_e}{(O.D_t - O.D_e) O.D_o}$ against t should give a straight line and the slope will give $\frac{k_1}{2.3} \left(\frac{O.D_o + O.D_e}{O.D_o - O.D_e} \right)$,

from which k_1 can be calculated. By carrying out an experiment at a high maleic acid concentration of LM it was possible to push reaction (13) to the right and fully form the maleic

acid complex; the spectrum of this species at 25° is a continuum with relatively little absorption at 387 mμ (ε = 400). This reaction at high maleic acid concentration was again very slow suggesting a rate independent of maleic acid concentration. The log plots for the data of figure 14 are shown in figure 15; the plots, however, show some curvature. Attempts to correct optical densities for the small contribution by the maleic acid complex gave essentially the same curved plots. The reason for the curvature is not too clear; it is possible that a similar scheme involving chloride displacement may be involved to some extent:



The important conclusion is that the complex formation process is clearly independent of the maleic acid concentration (plots 15(b) and (c) give the same k_1 although the maleic acid concentration differs by a factor of two and the reaction at high maleic acid concentration is again very slow). This shows the importance of the solvent assisted dissociation reaction. The slope of the final essentially linear portion of the log plots would yield the k_1 values summarized in Table XVI. The value of k_1 at 25° is about 3.0 times the value obtained from the "blank" reaction.

The K_M value for the complexing reaction with maleic acid is found to be $\sim 3000 \text{ M}^{-1}$ at 80°.

Summarized results for the complex formation reactions with maleic acid at different conditions

Conc. of $\text{Ir}(\text{CO})\text{Cl}(\text{PPh}_3)_2$ $\times 10^4 \text{ M}$	Conc. of maleic acid $\times 10^3 \text{ M}$	Temperature $^\circ\text{C}$	k_1^* $\times 10^4 \text{ Sec}^{-1}$
(a) 1.16	3.45	25 $^\circ$	0.36
(b) 0.58	3.45	25 $^\circ$	0.33
(c) 0.58	6.90	25 $^\circ$	0.3
(d) 1.16	3.45	40 $^\circ$	0.45
(e) 1.16	3.45	60 $^\circ$	0.55
(f) 0.58	3.45	80 $^\circ$	0.55

*Obtained from the linear portions of the log plots.

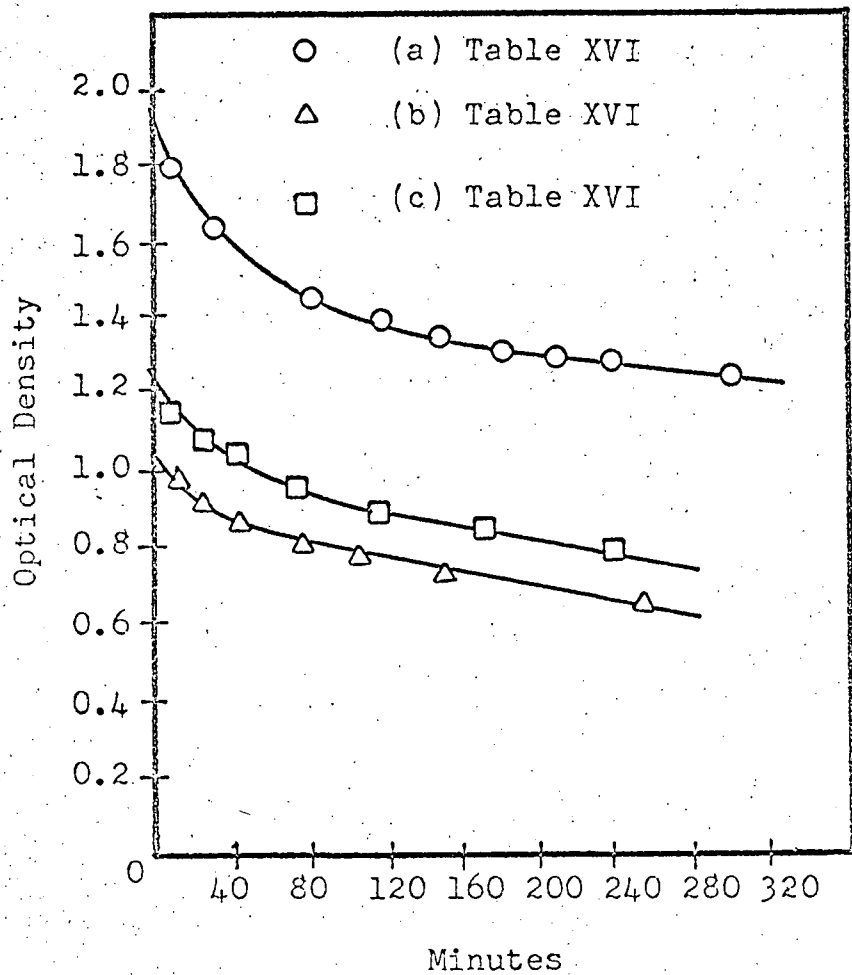


Figure 14: Plots of optical density against time for maleic acid complexing at different conditions

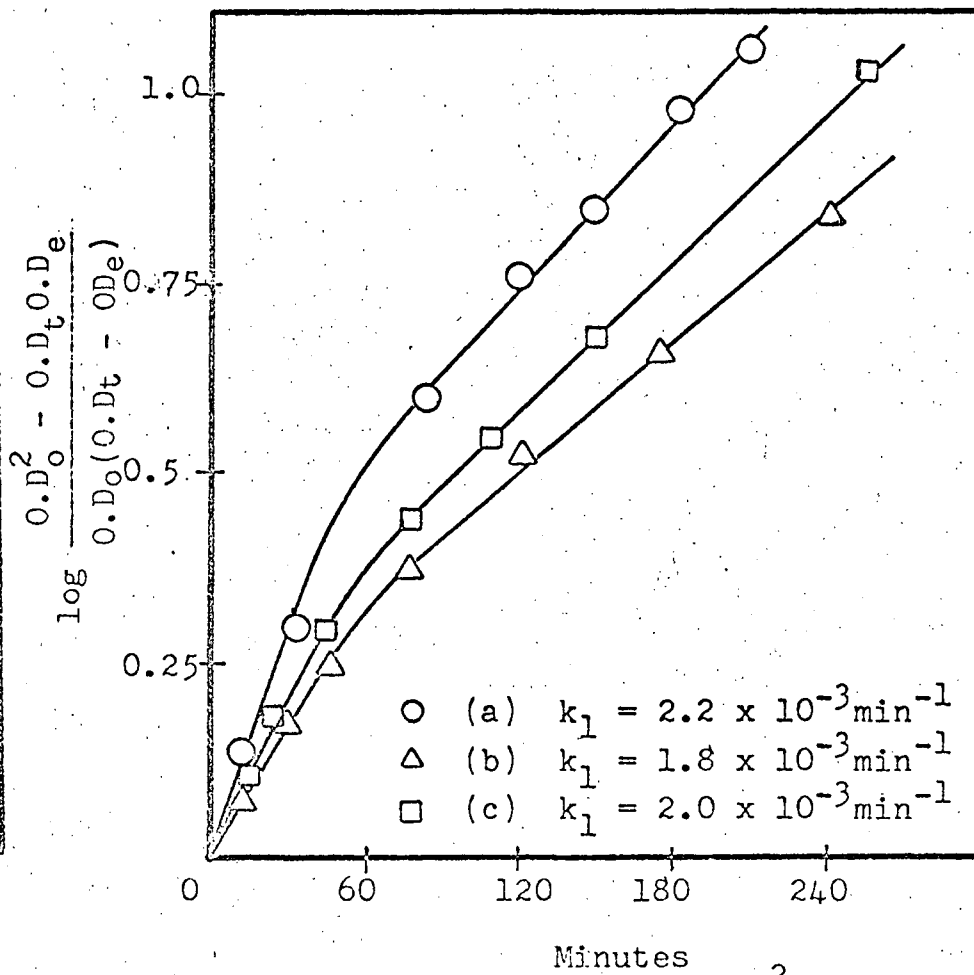
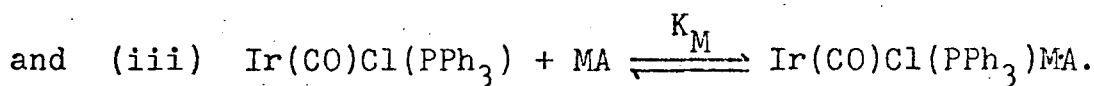
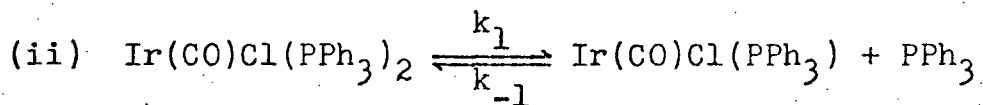
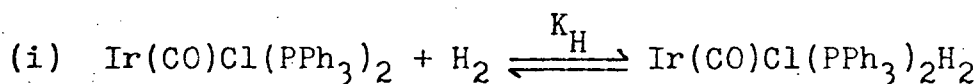


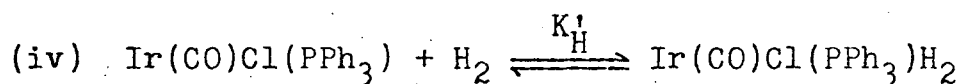
Figure 15: Plots of $\log \frac{0.D_o^2 - 0.D_t.O.D_e}{0.D_o(O.D_t - O.D_e)}$ against time for (a), (b) and (c) in figure

V. DISCUSSION

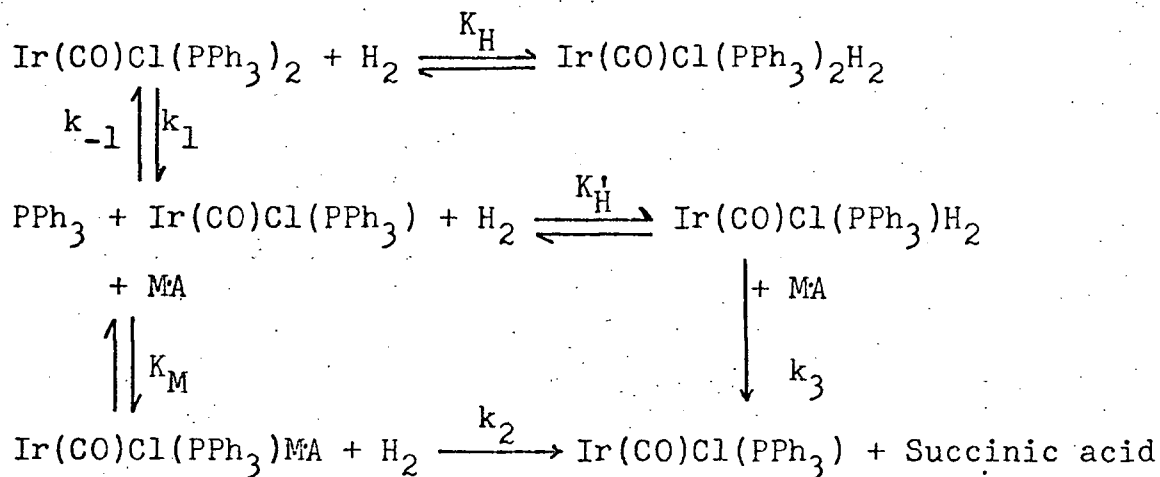
The spectrophotometric studies suggest that under the conditions of the hydrogenation reaction in DMA, i.e., 730 mm of hydrogen pressure and 80°, the following equilibria are present:



There is also a possibility of the reversible formation of the dihydride complex of the species, $\text{Ir}(\text{CO})\text{Cl}(\text{PPh}_3)$.



Taking into consideration all these equilibria and all the reaction paths that could be involved one can write the following scheme for the overall hydrogenation reaction:



The molecular dihydride, $\text{Ir}(\text{CO})\text{Cl}(\text{PPh}_3)_2\text{H}_2$, is rapidly formed in the system but the possibility of it reacting with the maleic acid as the process of hydrogenation is ruled out on the argument that (a) such a reaction would require a first order dependence of the rate on the iridium concentration, whereas such dependence is not observed; (b) no initial autocatalysis would be expected in the uptake plot, and (c) the hydrogenation reaction will not be inhibited by the excess triphenylphosphine as observed. The catalytic activity, therefore, results from the loss of a triphenylphosphine ligand from the original $\text{Ir}(\text{CO})\text{Cl}(\text{PPh}_3)_2$ complex in a relatively slow equilibrium step ($K = k_1/k_{-1}$). Therefore, initially the rate of hydrogen uptake increases autocatalytically and finally as the equilibrium between $\text{Ir}(\text{CO})\text{Cl}(\text{PPh}_3)_2$ and $\text{Ir}(\text{CO})\text{Cl}(\text{PPh}_3)$ species is reached the rate of hydrogen uptake approaches a maximum value. The fourth coordination position vacated by the loss of a triphenylphosphine group is probably occupied by a solvent molecule. The $\text{Ir}(\text{CO})\text{Cl}(\text{PPh}_3)$ species forms a complex with maleic acid in a relatively rapid equilibrium (K_M) which could then react with hydrogen (k_2 path). Thus, in this case, the maleic acid is activated by the iridium complex for further reaction with hydrogen to form succinic acid. Alternatively, the $\text{Ir}(\text{CO})\text{Cl}(\text{PPh}_3)$ species could react with molecular hydrogen in a rapid reversible reaction (K_H') forming a dihydride complex, $\text{Ir}(\text{CO})\text{Cl}(\text{PPh}_3)\text{H}_2$, which then

reacts with maleic acid (k_3 path) yielding the hydrogenated product.

If the hydrogenation reaction involves both paths (k_2 and k_3) simultaneously then the rate law will be of the form (for derivation see Appendix I):

$$\text{Rate} = \frac{(k_2 K_M + k_3 K'_H)[H_2][MA][Ir_{\text{total}}]}{1 + K_M[MA] + K'_H[H_2] + [PPh_3](1 + K_H[H_2])/K} \quad 19$$

where $K = k_1/k_{-1}$. The $k_2 K_M$ and $k_3 K'_H$ terms refer respectively to the k_2 and k_3 paths; $k_3 K'_H$ becomes negligible if the k_2 path predominates and vice versa. Thus the rate law can be simplified to

$$\text{Rate} = \frac{k_2 K_M [H_2][MA][Ir_{\text{total}}]}{1 + K_M[MA] + [PPh_3](1 + K_H[H_2])/K} \quad 20$$

if the reaction involves only the k_2 path. The spectrophotometric results supply the evidence for the formation of the $\text{Ir}(\text{CO})\text{Cl}(\text{PPh}_3)\text{MA}$ complex whereas the formation of the $\text{Ir}(\text{CO})\text{Cl}(\text{PPh}_3)_2$ complex, though a possibility, is neither supported nor discarded by the data we have. Similar mechanistic schemes can be written for the bromo and the iodo complexes $\text{Ir}(\text{CO})\text{Br}(\text{PPh}_3)_2$ and $\text{Ir}(\text{CO})\text{I}(\text{PPh}_3)_2$ and the rate law for the hydrogenation reactions in DMA catalysed by these complexes is the same as that for the chloro complex given by equations 19 and 20. These rate-laws agree at least qualitatively with the data observed for these three complexes. The rate-laws suggest between zero and first order

dependence on the iridium concentration; this is reflected in the $[\text{PPh}_3]/K$ term in the denominator which increases with the iridium concentration and thus giving a limiting rate at higher concentration. The data obtained for $\text{Ir}(\text{CO})\text{Cl}(\text{PPh}_3)_2$ and $\text{Ir}(\text{CO})\text{Br}(\text{PPh}_3)_2$ agree with this dependence although in the case of $\text{Ir}(\text{CO})\text{I}(\text{PPh}_3)_2$ a first order dependence on the iridium concentration is observed. This can be explained if greater dissociation of $\text{Ir}(\text{CO})\text{Cl}(\text{PPh}_3)_2$ (greater K) is assumed. The reactions are between zero and first order in hydrogen and maleic acid in agreement with the rate law. If the k_2 path is assumed to be the dominant hydrogenation step then a more quantitative analysis of the data can be made. An expression such as (20) is normally analyzed by writing the inverse function (rate^{-1}), for example,

$$\frac{1}{\text{Rate}} = \frac{1 + [\text{PPh}_3](1 + K_{\text{H}}[\text{H}_2])/K}{k_2 K_{\text{M}} [\text{H}_2] [\text{Ir}_{\text{total}}]} \cdot \frac{1}{[\text{MA}]} + \frac{1}{k_2 [\text{H}_2] [\text{Ir}_{\text{total}}]}$$

and plotting rate^{-1} against $[\text{MA}]^{-1}$ at constant $[\text{H}_2]$. However remembering that

$$[\text{PPh}_3] = [\text{Ir}(\text{CO})\text{Cl}(\text{PPh}_3)] + [\text{Ir}(\text{CO})\text{Cl}(\text{PPh}_3)\text{MA}]$$

it is readily shown that the $[\text{PPh}_3]/K$ term also varies with both maleic acid and hydrogen concentrations, and good linear inverse plots are not obtained. However, at sufficiently high maleic acid concentration the limiting rate

will be given by $k_2[\text{H}_2][\text{Ir}_{\text{total}}]$; figure 8 indicates a limiting value of about $5 \times 10^{-6} \text{ M Sec}^{-1}$ which gives $k_2[\text{H}_2] \approx 1 \times 10^{-3} \text{ Sec}^{-1}$. Taking a value of $3.5 \times 10^{-3} \text{ M atmos}^{-1}$ for the hydrogen solubility (quoted for dimethylformamide⁴¹) gives $k_2 \sim 0.3 \text{ M}^{-1} \text{ Sec}^{-1}$ at 80° . To give the curved dependence shown in figures 7, 8, 9 it is necessary that the three denominator terms $K_M[\text{MA}][\text{PPh}_3]/K$ and $K_H[\text{H}_2][\text{PPh}_3]/K$ be of comparable magnitude; that this is so can readily be shown by calculations over the range of concentrations used. It is possible to determine values of k_2 at 80° by using the rate expression (20) and calculating each of the terms involved; K_M was taken as 3000 M^{-1} , $K_H[\text{H}_2]$ as 0.6 and K as $1.3 \times 10^{-6} \text{ M}$. Some typical calculated values are summarized in the Table XVII. These calculated values are considered in reasonable agreement with the value estimated from the limiting rate particularly in view of the uncertainty associated with the equilibrium constants. Any absorption at $387 \text{ m}\mu$ by the $\text{Ir}(\text{CO})\text{Cl}(\text{PPh}_3)$ or $\text{Ir}(\text{CO})\text{Cl}(\text{PPh}_3)\text{MA}$ species (assumed to be negligible) could give considerable error in K and K_M and also the spectrophotometric data are obtained at concentrations of about one tenth those used in the gas uptake measurements.

The kinetic and equilibrium data could be consistent therefore with a hydrogenation step involving reaction of molecular hydrogen with an olefin complex formed from a slowly produced intermediate $\text{Ir}(\text{CO})\text{Cl}(\text{PPh}_3)$. However the

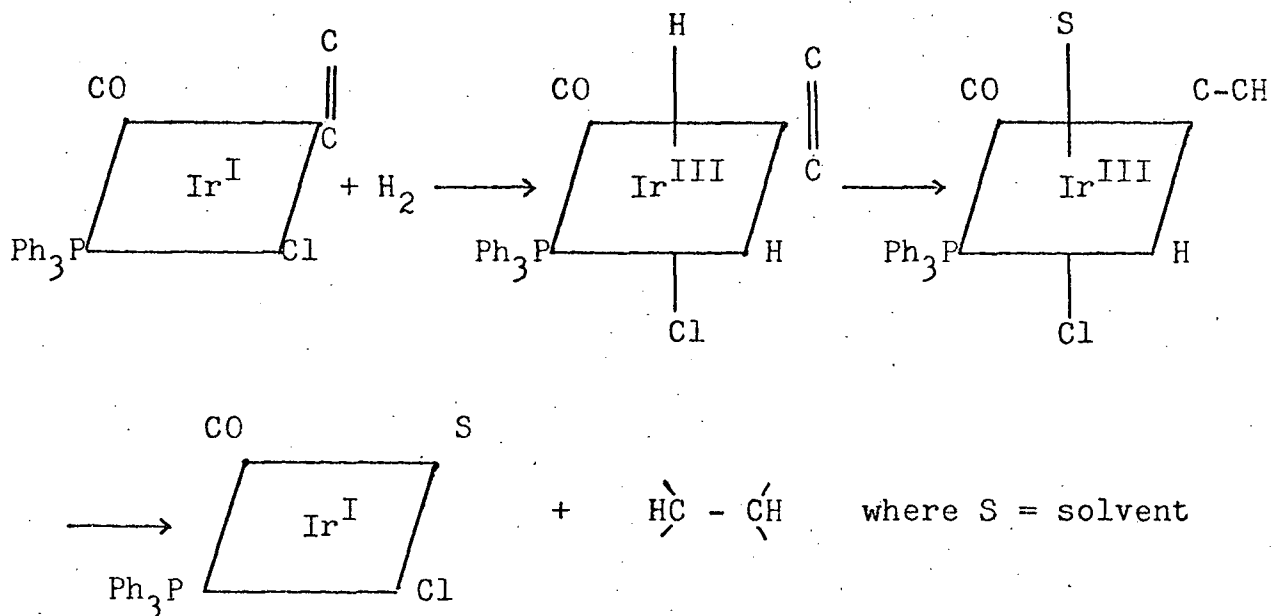
TABLE XVII

Summary of the data at 80°

$[\text{Ir}_{\text{total}}]$ $\times 10^3 \text{ M}$	$[\text{MA}]$ $\times 10^2 \text{ M}$	$[\text{PPh}_3]$ $\times 10^3 \text{ M}$	$\text{H}_2, \text{ mm}$	Rate $\times 10^6$ M Sec^{-1}	Calculated $k_2[\text{H}_2] \times 10^3 \text{ Sec}^{-1}$	$k_2, \text{M}^{-1} \text{ Sec}^{-1}$
5.36	7.0	0.87	730	4.00	4.5	1.3
2.68	7.0	0.59	730	2.9	4.8	1.4
1.34	7.0	0.39	730	2.0	4.9	1.4
5.36	3.5	0.63	730	2.5	3.9	1.1
5.36	2.0	0.487	730	2.4	3.7	1.0
5.36	1.0	0.31	730	1.7	4.3	1.2
5.36	7.0	0.96	365	1.45	1.49	1.0
5.36	7.0	1.01	186	1.1	1.0	1.1

alternate path of reaction of the olefin with a corresponding dihydride complex cannot be completely ruled out.

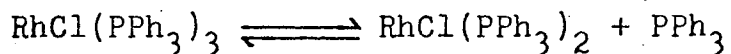
Mechanisms of catalytic hydrogenation have been discussed in detail by several workers^{4,5,17,42}. All systems must involve intermediate hydride species but it is not known whether coordination of the olefin as a π -bonded is a general feature. A plausible mechanism for the k_2 path suggested here is shown in the following scheme:



Hydride formation is accompanied by formal oxidation of the metal; hydrometallation of olefinic bonds (the second step) is well established, being an example of a much wider class of insertion reactions.

A system much in common with the one described here is the recent one reported by Wilkinson and coworkers⁵ on the hydrogenation catalyst $\text{RhCl}(\text{PPh}_3)_3$ in benzene solutions.

This system is somewhat simpler in that the dissociation step



is rapid even at 25° and lies essentially to the right giving a high catalytic activity. In this system, however, it seems that the k_3 path involving the reaction of $\text{RhCl}(\text{PPh}_3)_2\text{H}_2$ with the olefin is dominant. Both studies show the importance of the dissociation step in making available a coordination site in the transition metal complex.

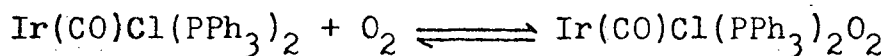
The efficiency of the catalyst is governed principally by the equilibrium constant K for the dissociation step; this is small (10^{-6} M at 80°) for the $\text{Ir}(\text{CO})\text{Cl}(\text{PPh}_3)_2$ complex. The first order dependence on the iridium concentration noted for the iodo complex indicates greater dissociation for this complex which would give rise to the increased catalytic activity. Other workers^{18,28} have reported increasing chemical reactivity of the $\text{Ir}(\text{CO})\text{X}(\text{PPh}_3)_2$ complexes in the order $\text{I} > \text{Br} > \text{Cl}$ in benzene solution where there is no measurable dissociation.

A lower rate of hydrogenation of fumaric acid could be explained by weaker complexing of this substrate with the solvated iridium species. This would correspond to a lower K_M value in the rate expression which would decrease the rate (consistent with this is the more rapid fall off in rate from the linear region for the fumaric acid systems; the term corresponding to $K_M[\text{MA}]$ would be smaller and the reaction

would be nearer first order in fumaric acid). More experiments are required to investigate the complexing with fumaric acid, but it is known that the fumaric acid complex of chlororuthenate (II) species is weaker than that of the corresponding maleic acid one.⁴

The catalytic activity of the $\text{Ir}(\text{CO})\text{Cl}(\text{PPh}_3)_2$ species in the different solvents is seen to decrease in the order dimethylacetamide > dimethylsulphoxide \gg benzene. Both the donor strength and solvating power of the solvents are likely to be important for this type of system. Good coordinating solvents enhance the solvent path for the associative trigonal-bipyramidal substitution mechanism of the square planar d^8 complexes (11). The rates of hydrogen addition to $\text{Ir}(\text{CO})\text{X}(\text{PPh}_3)_2$ complexes and the hydrogenation rates catalysed by the $\text{RhCl}(\text{PPh}_3)_3$ complex are increased by the use of more polar solvents^{5,28} and these findings have been interpreted in terms of reaction through a highly polar transition state. Generally the donor strength and solvating power of dimethylacetamide and dimethylsulphoxide are thought to be very similar⁴³.

The reason for the marked increase in the hydrogenation rate in the presence of small amounts of oxygen is not understood. The known equilibrium



is presumably involved, and the oxygen adduct is known to be light sensitive giving as yet unidentified products.¹⁷

APPENDIX I

I. If the reaction involving both paths k_2 and k_3 simultaneously is considered the rate expression can be derived as follows:

Rate of hydrogen uptake =

$$k_2[H_2][\text{Ir}(\text{CO})\text{Cl}(\text{PPh}_3)\text{MA}] + k_3[\text{Ir}(\text{CO})\text{Cl}(\text{PPh}_3)_2\text{H}_2][\text{MA}] \quad (\text{a})$$

$$\left. \begin{aligned} \text{and also } [\text{Ir}(\text{CO})\text{Cl}(\text{PPh}_3)\text{MA}] &= K_M[\text{MA}][\text{Ir}(\text{CO})\text{Cl}(\text{PPh}_3)] \\ \text{and } [\text{Ir}(\text{CO})\text{Cl}(\text{PPh}_3)_2\text{H}_2] &= K_H[\text{H}_2][\text{Ir}(\text{CO})\text{Cl}(\text{PPh}_3)] \end{aligned} \right\} \quad (\text{b})$$

Substitution of (b) into (a) gives

Rate

$$\begin{aligned} &= k_2 K_M [\text{H}_2][\text{MA}][\text{Ir}(\text{CO})\text{Cl}(\text{PPh}_3)] + k_3 K_H' [\text{MA}][\text{H}_2][\text{Ir}(\text{CO})\text{Cl}(\text{PPh}_3)] \\ &= (k_2 K_M + k_3 K_H') [\text{H}_2][\text{MA}][\text{Ir}(\text{CO})\text{Cl}(\text{PPh}_3)] \end{aligned} \quad (\text{c})$$

$$\begin{aligned} [\text{Ir}_{\text{total}}] &= [\text{Ir}(\text{CO})\text{Cl}(\text{PPh}_3)_2] + [\text{Ir}(\text{CO})\text{Cl}(\text{PPh}_3)\text{MA}] + \\ &\quad [\text{Ir}(\text{CO})\text{Cl}(\text{PPh}_3)] + [\text{Ir}(\text{CO})\text{Cl}(\text{PPh}_3)_2\text{H}_2] + \\ &\quad [\text{Ir}(\text{CO})\text{Cl}(\text{PPh}_3)\text{H}_2] \end{aligned} \quad (\text{d})$$

$$\left. \begin{aligned} [\text{Ir}(\text{CO})\text{Cl}(\text{PPh}_3)_2] &= [\text{PPh}_3][\text{Ir}(\text{CO})\text{Cl}(\text{PPh}_3)]/K \\ [\text{Ir}(\text{CO})\text{Cl}(\text{PPh}_3)_2\text{H}_2] &= K_H[\text{H}_2][\text{PPh}_3][\text{Ir}(\text{CO})\text{Cl}(\text{PPh}_3)]/K \end{aligned} \right\} \quad (\text{e})$$

$$\text{and } [\text{Ir}(\text{CO})\text{Cl}(\text{PPh}_3)\text{H}_2] = K_H'[\text{H}_2][\text{Ir}(\text{CO})\text{Cl}(\text{PPh}_3)]$$

Substitution from (e) and (b) into (d) gives

$$[\text{Ir}_{\text{total}}] = [\text{Ir}(\text{CO})\text{Cl}(\text{PPh}_3)] \left\{ 1 + K_M[\text{MA}] + K_H'[\text{H}_2] + [\text{PPh}_3](1 + K_H[\text{H}_2])/K \right\}$$

Therefore:

$$[\text{Ir}(\text{CO})\text{Cl}(\text{PPh}_3)] = [\text{Ir}_{\text{total}}] / \left\{ 1 + K_M[\text{MA}] + K_H'[\text{H}_2] + [\text{PPh}_3](1 + K_H[\text{H}_2])/K \right\} \quad (\text{f})$$

Substitution of (f) into (c) gives

$$\text{Rate} = \frac{(k_2 K_M + k_3 K_H') [\text{H}_2] [\text{MA}] [\text{Ir}_{\text{total}}]}{1 + K_M[\text{MA}] + K_H'[\text{H}_2] + [\text{PPh}_3](1 + K_H[\text{H}_2])/K}$$

REFERENCES

1. L. Vaska and J.W. Diluzio, J. Am. Chem. Soc., 84, 679 (1962); 83, 2784 (1961).
2. J. Halpern, Am. Rev. Phys. Chem., 16, 103 (1965) and the references therein.
3. J. Halpern, Proc. 3rd Int. Cong. Catalysis Amsterdam, 1964; North Holland, Amsterdam, 1965, p. 146.
4. J. Halpern, J.F. Harrod and B.R. James, J. Am. Chem. Soc., 88, 5750 (1966).
5. J.A. Osborn, F.H. Jardine, J.F. Young and G. Wilkinson, J. Chem. Soc., 1711 (1966) and references therein.
6. J. Halpern, J.F. Harrod and S. Ciccone, Can. J. Chem., 39, 1372 (1961).
7. J. Halpern and B.R. James, Can. J. Chem., 44, 671 (1966).
8. M. Calvin and W.K. Wilmarth, J. Am. Chem. Soc., 78, 1301 (1956).
9. J. Halpern, Adv. in Catalysis, XI, 301 (1959).
10. J. Halpern, J.F. Harrod and B.R. James, J. Am. Chem. Soc., 83, 753 (1961).
11. R.D. Cramer, E.L. Jenner, R.V. Lindsey, Jr. and U.G. Stolberg, J. Am. Chem. Soc., 85, 1691 (1963).
12. J. Kwiatek, I.L. Mador and J.K. Seyler, "Reactions of coordinated ligands and Homogeneous Catalysis," Advances in Chemistry Series, No. 37, Am. Chemical Society, Washington, D.C. (1963).
13. L. Simandi and F. Nagy, Proc. Symp. Coord. Chem., Tihany, Hungary, 329 (1964).
14. B.R. James and G.L. Rempel, Can. J. Chem., 44, 233 (1966) and unpublished results.
15. L. Marko, Chem. Ind. (London), 260 (1962).

16. E.N. Frankel, E.A. Emken, H.M. Peters, V.L. Dandson and R.O. Betterfield, *J. Org. Chem.*, 29, 3292 (1964).
17. L. Vaska, *Inorg. Nucl. Chem. Letters*, 1, 89 (1965).
18. L. Vaska and R.E. Rhodes, *J. Am. Chem. Soc.*, 87, 4970 (1965).
19. J. Kwaitek and J.K. Seyler, *Proc. Intern. Conf. Coord. Chem.*
20. J. Chatt and B.L. Shaw, *J. Chem. Soc.*, 5075 (1962).
21. H.C. Clarke and W.S. Tsang, *Chem. Commun.*, 123 (1966).
22. P.M. Treichel, E. Pitcher and F.G.A. Stone, *Inorg. Chem.*, 1, 511 (1962).
23. M.J. Mays and G. Wilkinson, *Nature*, 1167 (1964).
24. D.N. Lawson, M.J. Mays and G. Wilkinson, *J. Chem. Soc. (A)*, 52 (1966).
25. M.C. Baird, D.N. Lawson, J.T. Mague, J.A. Osborne and G. Wilkinson, *Chem. Commun.*, 129 (1966).
26. R.F. Heck, *Adv. Chem. Series*, Vol. 49, Am. Chem. Soc., Washington, D.C., 181 (1965).
27. B.R. James and A. McClaughlin, Unpublished results.
28. J. Halpern and P.B. Chock, *J. Am. Chem. Soc.*, 88, 3511 (1966).
29. J.P. Collman and W.R. Roper, *J. Am. Chem. Soc.*, 87, 4008 (1965); 88, 480 (1966) and references therein.
30. L. Vaska and S.S. Bath, *J. Am. Chem. Soc.*, 88, 1333 (1966) and references therein.
31. R.S. Nyholm and K. Vrieze, *J. Chem. Soc.*, 5337 (1965).
32. J.P. Collman and J.W. Kang, *J. Am. Chem. Soc.*, 88, 3459 (1966); 89, 844 (1967).
33. L. Vaska, *Science*, 140, 809 (1963).
34. S.J. LaPlaca and J.A. Ibers, *J. Am. Chem. Soc.*, 87, 2581 (1965).

35. R. Cramer and G.W. Parshall, J. Am. Chem. Soc., 87, 1392 (1965).
36. W.H. Baddley, J. Am. Chem. Soc., 88, 4545 (1966).
37. L. Vaska, Science, 152, 769 (1966).
38. F.D. Mango and I. Dvoretzky, J. Am. Chem. Soc., 88, 1654 (1966).
39. B.R. James and A. McLaughlin, unpublished results.
40. A.A. Frost and R.G. Pearson, Kinetics and Mechanism, pp. 186-187, John Wiley & Sons, Inc., New York.
41. Dupont product information bulletin. A Review of Catalytic and Synthetic Applications for DMF and DMA.
42. J. Halpern, Chem. Eng. News, 44 (45), 68 (1966).
43. V. Gutmann, R.S. Drago, Papers presented at Conference on Non-Aqueous Solvent Chemistry. Hamilton, June 1967.